5 Clinical Applications of Nuclear Cardiology

Maria João Vidigal Ferreira
and Manuel D. Cerqueira

5.1 Introduction

Radionuclide techniques are used for cardiovascular imaging to assess perfusion, function, metabolism, innervation, and infarction [1–3]. Single-photon emission computed tomographic (SPECT) techniques prevail relative to the use of planar or positron emission tomography (PET). With SPECT there is an extensive body of literature supporting efficacy and prognostic value in a wide variety of clinical scenarios. As practiced in the United States and Europe, myocardial perfusion imaging (MPI) using SPECT or PET predominates and accounts for the majority of nuclear cardiology procedures. This concise clinical overview will mainly focus on the assessment of myocardial perfusion, viability, and left ventricular function. Imaging of myocardial sympathetic innervation, infection, inflammation, and infiltrative diseases that involve the myocardium will also be addressed.

M. J. V. Ferreira
Faculty of Medicine, Coimbra Hospital and University Center, University of Coimbra, Coimbra, Portugal

M. D. Cerqueira (✉)
Department of Nuclear Medicine, Cleveland Clinic, Cleveland, OH, USA

Cleveland Clinic Lerner College of Medicine, Of Case Western Reserve University, Cleveland, OH, USA
e-mail: cerquem@ccf.org

5.2 Historical Perspective of Nuclear Cardiology

MPI has evolved over more than 50 years to the point where it can now provide diagnostic and prognostic information in nearly all patient groups. Early studies were performed with K-43 in animal models and in man, but it was only with the availability of thallium-201 (Tl-201) in the mid-1970s that the technique using planar imaging became widely utilized for detecting the presence and extent of coronary artery disease (CAD). A decade later single-photon emission computed tomography, SPECT, was introduced and rapidly became the predominate method of acquisition. Since not all patients were capable of exercising, the use of pharmacologic stress, either with vasodilators or inotropic positive agents, allowed perfusion studies to be performed in nearly all patients. It also became evident that Tl-201 was not the ideal perfusion tracer and the availability of technetium-99m (Tc-99m)-labeled perfusion tracers, sestamibi (late 1980s) and tetrofosmin (late 1990s), improved image quality and reduced radiation exposure. These two tracers now account for the majority of perfusion studies. Perfusion imaging was shown not only to be capable of diagnosing the presence or absence of CAD but also to provide accurate information on risk assessment and prognosis. By the late 1980s, ECG-gated acquisition of perfusion images was developed and the

H. Ahmadzadehfar et al. (eds.), *Clinical Nuclear Medicine*,
https://doi.org/10.1007/978-3-030-39457-8_5

simultaneous assessment of perfusion and left ventricular global and regional function became an important tool in the diagnosis and management of CAD.

PET cardiac applications have been available since the early 1980s but were performed at a limited number of tertiary referral centers. With the development of PET/CT systems and greater availability of Rb-82 generators and on-site cyclotrons to produce N-13 for ammonia synthesis, cardiac PET achieved greater clinical penetration. PET tracers and imaging systems show clear advantages over SPECT. The high-energy emitted photons and the shorter half-life of the different tracers provide higher-quality images with reduced radiation exposure. Evaluation of perfusion and myocyte metabolism using F-18 fluorodeoxyglucose (FDG) are important features in the detection and risk stratification of CAD, and in the last decades, PET has been increasingly used for these purposes.

There have also been significant advances in SPECT systems with high-sensitivity detectors and hybrid CT systems for attenuation correction becoming available for improved image quality. Despite the higher cost of such systems, the advantages related to lower radiation exposure and better image quality offer significant advantages over older systems. Nuclear cardiology has advanced beyond perfusion imaging, assessment of function, and viability and is now providing clinical valuable information on the cardiac sympathetic nervous system, myocardial inflammation, and infiltrative diseases and infection. The future looks very promising for an established modality that has continued to be innovative in answering today's clinical needs for the evaluation and management of all types of cardiac patients.

5.3 Perfusion Imaging

5.3.1 Basic Concepts

Myocardial blood flow to the myocardium is through large epicardial conduit vessels, which offer almost no resistance to blood flow, intermediate arterioles that regulate resistance, and the extensive intramyocardial microcirculation which deliver nutrients and oxygen to the myocytes. Increases in myocardial work and, thus, in energy demands are accompanied by an increase in myocardial blood flow facilitated by a decrease in small vessel resistance due to the vasodilation mediated by several endothelium-dependent factors.

In the presence of dynamically significant large epicardial coronary vessel stenosis (≥50–80%), the site of resistance moves from the small vessels to the stenotic vessel. As long as there is adequate compensatory downstream vasodilation and decreased resistance, resting blood flow will be enough to meet myocardial energy demand. With progression of a coronary stenosis, the small vessel dilation capacity increases to maintain myocardial perfusion. Following exercise or pharmacologic stress, blood flow increases in the myocardium with normal coronary arteries, but in those perfused by arteries with a critical luminal stenosis (50–90% lumen stenosis) or endothelial dysfunction, a failure to increase or even a decrease of blood flow may occur resulting in symptoms of ischemia and a heterogeneity in myocardial blood flow that can be measured by flow tracers [4].

Given the above framework, MPI requires the comparison of images acquired in the resting state and after dynamic exercise or pharmacologic stress. Heterogeneous radiotracer uptake reflects abnormal blood flow caused by a coronary anatomic or functional abnormality. Ischemia is characterized by areas of reduced or absent uptake of the perfusion tracer on stress images with normal uptake on rest images (reversible defect), while myocardial scar has diminished uptake on both stress and rest images (fixed defect). Areas of normal myocardium have a homogeneous distribution of the perfusion tracer on both sets of images (stress and rest).

5.3.2 Radiopharmaceuticals and Imaging Protocols

The following sections will describe the characteristic of each of the cardiac

radiopharmaceuticals and how they are used in the most commonly performed imaging protocols. The recommendations are based on the published guidelines [2, 3, 5].

5.3.2.1 Thallium-201

Tl-201 is a K+ analog that is transported across cell membranes by the Na/K ATPase system [6]. Initial myocardial uptake is proportional to blood flow over a wide physiological range and is dependent on the presence of viable myocardial cells. Following the rapid high initial myocardial uptake, Tl-201 re-equilibrates with the lower concentration in the blood in a time-dependent fashion. This is called redistribution and like the initial uptake is directly proportional to blood flow to the area and the presence of functioning myocytes. Tl-201 can also be used to identify viable myocardium through delayed uptake representing eventual K+ concentrations in the myocytes [7]. The high and nearly linear initial myocardial uptake following stress makes Tl-201 a better marker of myocardial blood flow and then the Tc-99m tracers which have a lower extraction fraction across the coronary bed and plateau at lower flow rates. Tl-201 uptake and redistribution over time is a marker of the K+ blood pool and of viable myocardium. In areas where blood flow is severely reduced following stress, there may be very low uptake of Tl-201, initially, despite the presence of living myocytes. Even the 3–4 h redistribution images may still be abnormal in areas with living and viable myocytes. However, over 18–24 h or following reinjection of an additional dose to boost blood levels, if there are viable myocytes, with an intact Na/K ATPase system, Tl-201 is eventually taken up, and these areas will be clearly identified as hibernating myocardium and not infarction. The major disadvantages of Tl-201 are the low energy of the photons (69–83 KeV), easily attenuated by the tissues around the heart, and the long half-life (72 h) which give a high radiation exposure [6]. The effective radiation dose for this radiotracer is approximately 4.4 mSv per 37 MBq (1 mCi), and for these reasons, the routine use of Tl-201 to assess perfusion is no longer advised [2].

Figure 5.1 has four rows that identify all the possible combinations for identification of ischemia, infarction, and hibernating myocardium using Tl-201. In the typical imaging sequence using Tl-201, shown in the top row of Fig. 5.1, the patient is stressed with dynamic exercise or pharmacologic stress and 111–148 MBq (3–4 mCi) of Tl-201 injected at peak stress. The patient must be imaged within 10–15 min of completion of stress to avoid early redistribution and a resulting decrease in sensitivity. If the post-stress images are completely normal after physician review, the rest study is optional. If the stress images are not reviewed or are abnormal, this is followed 2.5–4 h later by a redistribution set of images. If the stress and redistribution images are normal, there is no ischemia or infarction, and there is no need to look for hibernation. If the stress images are abnormal and the redistribution images are normal, there is ischemia. When perfusion defects are present on the redistribution images, most likely this is scarred myocardium. However, if a clinical question of hibernating myocardium remains, there are several options for using Tl-201 as a marker of viable myocardium (Rows 2, 3, and 4, Fig. 5.1). The major disadvantages of Tl-201 are the low energy of the photons (69–83 KeV), easily attenuated by the tissues around the heart, and the long half-life (72 h) which gives a high radiation exposure [6] [2].

Assessment of viability is especially important in patients with congestive heart failure, known cardiomyopathies, or myocardial infarction [8]. In patients where myocardial viability assessment is of critical clinical importance and PET or cardiac MRI are not available, several approaches using Tl-201 can be used to further improve on the accuracy of the regular 4-h stress/redistribution sequence. These approaches include delayed imaging at 24 h (Row 1, Fig. 5.1). The patient may also be reinjection with 37 MBq of Tl-201 immediately following the redistribution images with imaging 15 min later (Row 2, Fig. 5.1) or imaging at 24 h (Row 3, Fig. 5.1). Both of these approaches result in three separate sets of images. Alternatively, Row 4, Fig. 5.1, four sets of images may be acquired. A rest/3–4-h

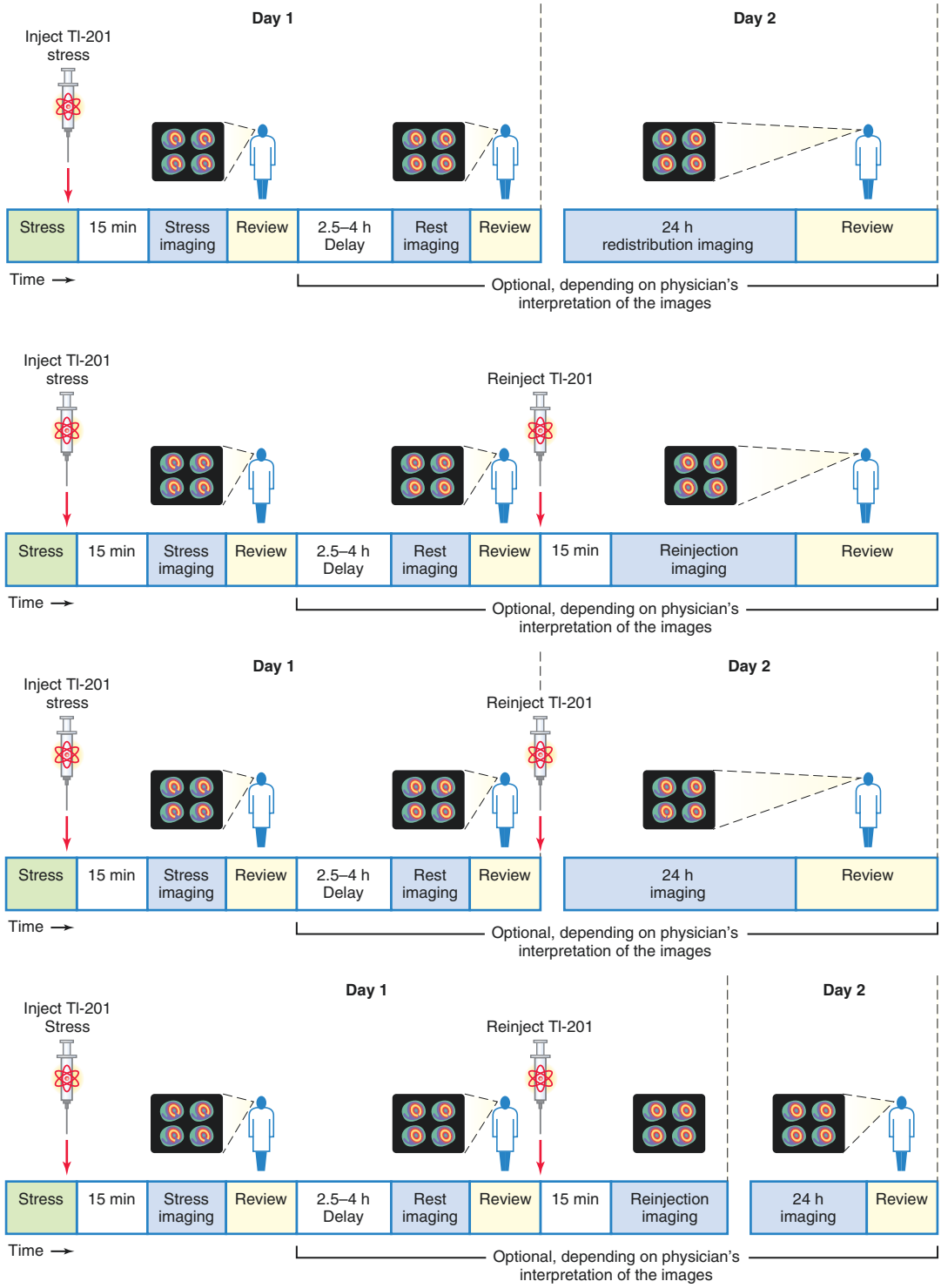

Fig. 5.1 Tl-201 protocols for detection of ischemia and viable myocardium

redistribution Tl-201 protocol can also be used for viability assessment, but this does not provide information on ischemia.

With the dual isotope approach, both ischemia and hibernation can be identified, but this procedure is no longer recommended, due to higher radiation exposure and increase rate of false-positive results for ischemia, as rest and stress images are obtained with different tracers, unless there is a clear indication to assess perfusion and viability in elderly patients that require shorter protocols or in the case that alternative methods are not available [2].

5.3.2.2 Technetium-99m Radiotracers

Tc-99m tracers were developed to overcome the limitations of Tl-201. Only two Tc-99m tracers are in clinical use: Tc-99m sestamibi (Cardiolite™) and Tc-99m tetrofosmin (Myoview™) [6]. The monoenergetic 140 keV higher energy of Tc-99m versus the 69–83 keV range of Tl-201 results in improved image resolution with less overall attenuation and scatter during imaging. Tc-99m has a half-life of 6 h in comparison to the 72 h of Tl-201. The shorter half-life allows administration of a higher Tc-99m dose resulting in high-count images. As an example, 148 MBq (4 mCi) f Tl-201 is administered compared to 444–1110 MBq (12–30 mCi) of the Tc-99m radiotracers. The higher counts obtained with a Tc-99m radiopharmaceutical and the lack of redistribution allows ECG-triggered gated acquisition for assessment of function. The minimal redistribution of Tc-99m tracers following injection allows greater flexibility as to when acquisition can be performed, as soon as 10 min or as far out as 4 h following stress. The whole-body effective dose is approximately 0.3 mSv per 37 MBq (1 mCi) of Tc-99m [2].

5.3.2.3 Tc-99m Sestamibi and Tetrofosmin

Both are monovalent cations which make them very lipophilic and facilitate entry into cells. Uptake is dependent on blood flow, plasma- and mitochondrial-derived membrane electrochemical gradients, cellular pH, and intact energy pathways [6]. Chemical or structural conversion of the molecule is not required, and unlike Tl-201 inhibitors of Na+, K+ and Ca2+ transport do not prevent uptake or retention in myocytes. Once inside the myocyte, they remain trapped with the greatest concentration in the mitochondria, and there is minimal washout. Following intravenous injection, they are cleared from blood by the liver, concentrated in the gall bladder, and excreted through the common bile duct into the GI tract. The initial high liver uptake does not allow the inferior wall to be seen clearly early post-injection and requires waiting 15–45 min following resting or pharmacologic stress injection to get adequate visualization. Clearance post-dynamic exercise is faster, and image acquisition can be started as soon as 10–20 min following injection [2, 6]. Tetrofosmin has the advantage to allow earlier scanning because of its lower hepatic uptake.

5.3.2.4 Tc-99m Radiotracer Imaging Protocol Options

The uptake and clearance characteristics of Tc-99m sestamibi and tetrofosmin are sufficiently similar that recommendations for imaging are identical with minor variation between injection time and when to image due to differences in liver clearance between the two tracers. In general Tc-99m tetrofosmin can be imaged sooner after injection.

Protocol options include a 2-day protocol, a 1-day split dose protocol (rest/stress, Fig. 5.2, or stress/rest sequence, Fig. 5.3),s and a dual isotope approach (Fig. 5.4) using Tl-201 at rest. The diagnostic accuracy results in the literature did not report significant differences between the various protocols or between these agents and Tl-201 [1, 2].

In the 2-day protocol (bottom rows of Figs. 5.2 and 5.3) the maximal dose of Tc-99m, 740–1110 MBq (20-30 mCi), is used for both images and provides high counts and better image quality. This protocol is optimal in obese patients and allows higher counts and accurate rest EF to be calculated as well a post-stress measurement which provides additional value. Due to time delays in getting test results and patient inconvenience, this protocol is not used widely. When

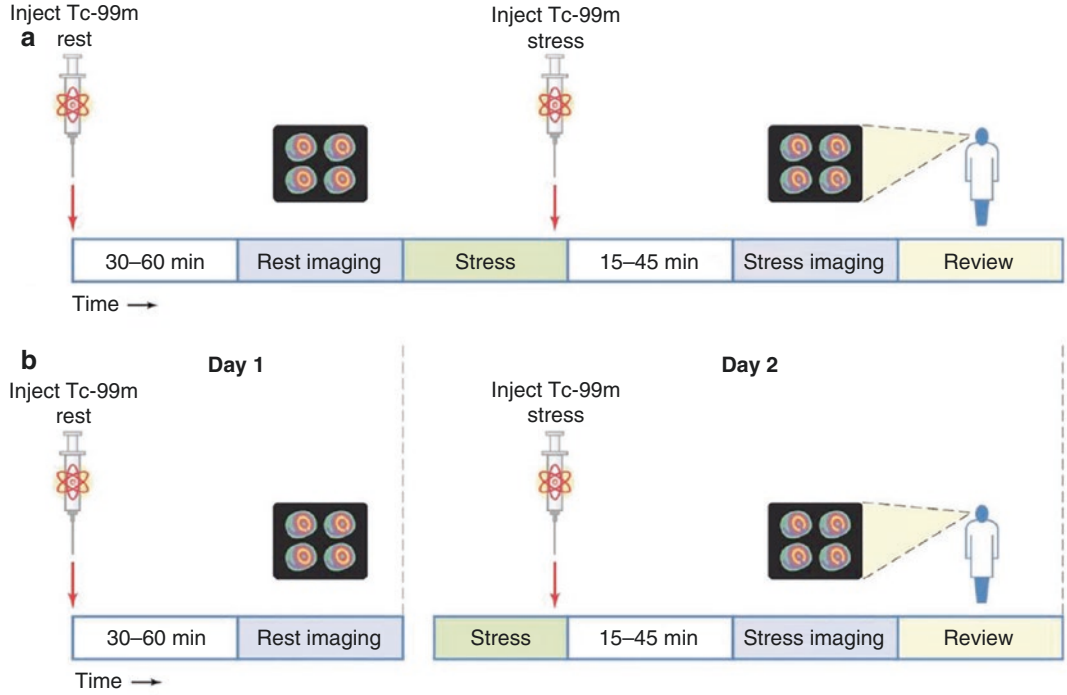

Fig. 5.2 Tc-99m 1- and 2-day stress/rest protocols

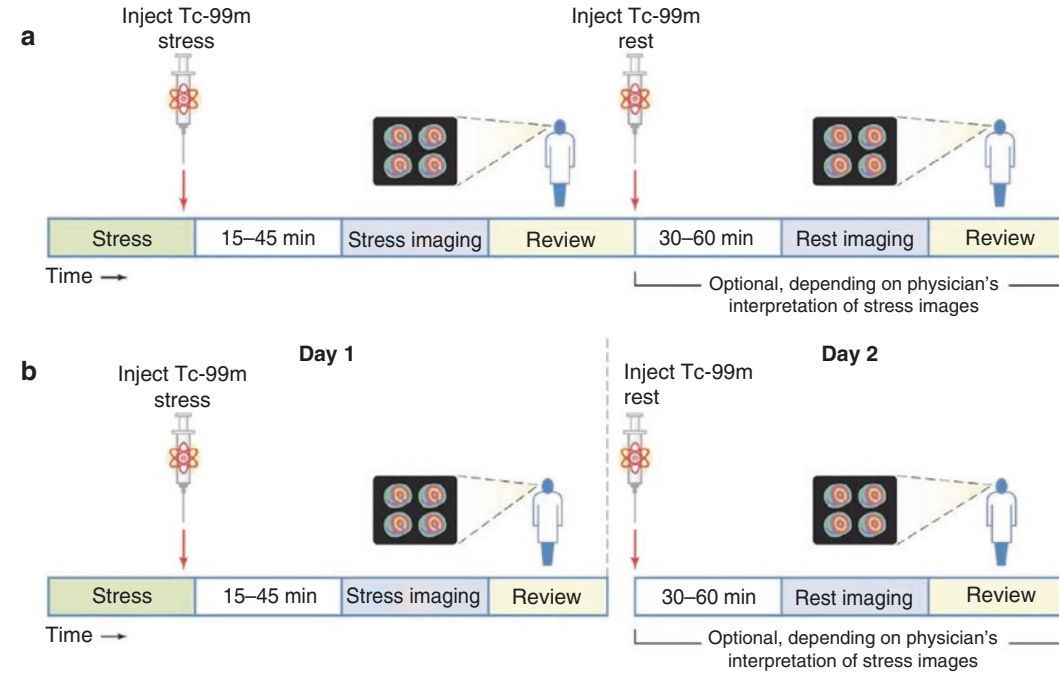

Fig. 5.3 Tc-99m 1- and 2-day rest/stress protocols

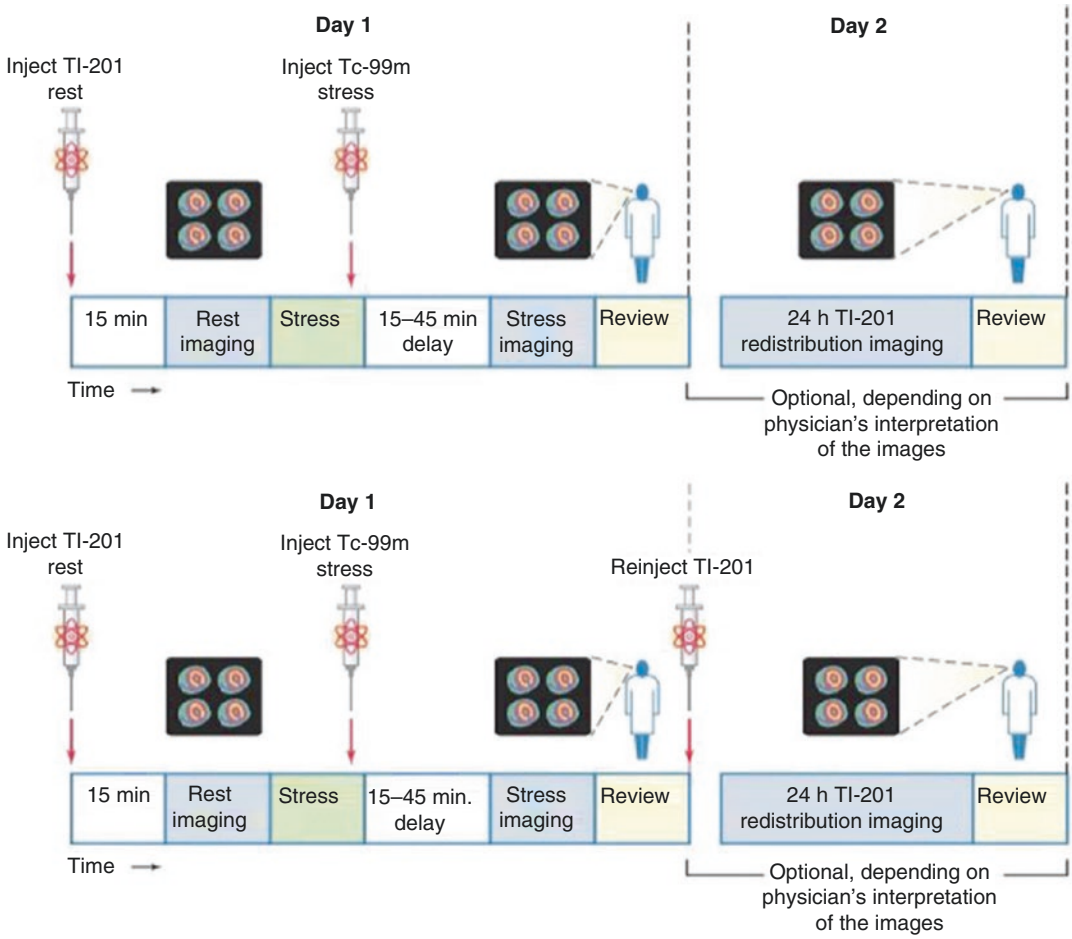

Fig. 5.4 Dual isotope rest Tl-201 and stress Tc-99m stress protocols with optional delayed redistribution and reinjection of Tl-201 for 24-h viability assessment

doing a 2-day protocol, the stress study should be done first, and if normal the resting study is not needed. Stress first provides results sooner and has a lower radiation exposure, especially if the stress is normal and the rest portion is not performed. In obese patients with soft tissue attenuation and low counts, gating and attenuation correction improves specificity and decreases the number of patients needing to return for a rest study [9].

For logistical reasons, 1-day stress and rest studies are usually performed as shown in top rows of Figs. 5.2 and 5.3. This requires administration of a low dose, 1/3 of the total dose or 296–444 MBq (8–12 mCi) for the first study, and a larger dose, 2/3 of the total dose or 740–1110 MBq (20–30 mCi), for the second study and waiting as long as possible between studies, usually 1.5–2.5 h, to allow for physical decay of Tc-99m. Using this approach, when the second set of images is acquired there is relatively little contamination from the first injection. The 1-day rest/stress sequence, shown in Fig. 5.2, is the most frequently performed protocol in the United States. The disadvantage of this sequence is that the low dose is given at rest when blood flow is lowest and there will be less myocardial tracer uptake. The higher stress dose, administered when blood flow is maximal, will give higher counts and better quality images. The gated post-stress image in patients with extensive ischemia may give a lower EF, due to residual myocardial

stunning, and then a true resting ejection fraction [10]. In patients with ischemia, a lower post-stress EF is a better predictor of higher cardiac death and infarction rate and then the size and severity of the defect alone [11]. The 1-day stress/rest protocol in upper row of Fig. 5.3 gives the lower dose when myocardial blood flow is the highest, during stress, and background activity in the subdiaphragmatic area is low due to a decrease in mesenteric blood flow associated with stress. With this protocol, if the stress images are normal, the rest study is not needed, improving laboratory efficiency and reducing radiation exposure [12–14]. Stress-first and stress-only protocols, whether in a 1- or 2-day sequence, are efficient and reduce radiation exposure. They require physician review of the stress images in order to make a decision on the need for a resting study the same or the following day.

The timing and sequence for a Tl-201/Tc-99m radiotracer dual isotope separate acquisition protocol is displayed in Fig. 5.4. For the resting Tl-201 study, the patient should be fasting and a dose of 111–148 MBq (3–4 mCi) of Tl-201 injected. Imaging should be delayed for 10–15 min. For stress, the patient is injected with 240–1110 MBq 740–1110 MBq (20–30 mCi) of a Tc-99m tracer. The separate acquisition approach takes advantage of the two distinct and separate energy levels of Tl-201 and Tc-99m. During the second acquisition, the gamma camera selectively acquires data centering on the higher energy Tc-99m window. Although, there is residual Tl-201 present from the resting study, the lower energy Tl-201 photons are excluded by using the higher Tc-99m window. When using the dual isotope approach and myocardial viability is in question, a rest-4-h redistribution Tl-201 study may be performed prior to performing the stress study [15]. Patients can also be injected with Tl-201 the evening before to give an approximate 12-h Tl-201 acquisition the following morning. This is an alternative method for the identification of myocardial viability, as mentioned above [2]. When the Tc-99m stress study has already been performed and questions of viability remain, delayed Tl-201 imaging cannot be performed on the same day due to the down scatter of the Tc-99m into the Tl-201 energy window. If both the rest and stress images have fixed perfusion defects, viability assessment can be performed with reinjection of 37 MBq (1 mCi) of Tl-201. In such situations, the patient may return at 24 h for Tl-201 viability imaging by which time there has been sufficient decay of the Tc-99m to allow uptake of the K+ properties of Tl-2-1 (Fig. 5.4).

5.3.3 Perfusion Tracers and Protocols for PET

Assessment of myocardial perfusion has been established as an important tool in the diagnosis and prognosis of coronary artery disease. SPECT has been one of the most used techniques for this purpose. PET improves the functional evaluation of CAD as it shows higher diagnostic accuracy and it allows measurements of myocardial blood flow (MBF) in absolute terms (milliliters per gram per minute). Quantification of MBF extends the conventional perfusion imaging to the detection of microvascular disease and balanced ischemia [3, 16].

PET tracers use positron emitting radionuclides, such as oxygen-15 (O-15), nitrogen-13 (N-13), rubidium-82 (Rb-82), or fluoride-18 (Fl-18). Due to their short half-lives, oxygen-15 water and N-13 ammonia studies are limited or best performed in centers with an on-site cyclotron. All PET tracers can be used with pharmacologic stress. Only N-13 ammonia and F-18 flurpiridaz can be used with dynamic exercise stress. Positrons are positively charged particles, emitted by the nuclei of unstable isotopes during radioactive decay. They interact with electrons, and annihilation occurs with the emission of two 511 KeV photons that travel in exactly 180° opposite directions. As PET detectors are placed in a ring surrounding the patient, events with temporal coincidence photons are located by opposing detectors. This result in an improved spatial and temporal resolution compared to SPECT, offering lower radiation exposure due to the very short half-lives of the radioisotopes with higher diagnostic accuracy.

Table 5.1 compares PET with SPECT MPI, pointing out the advantages and disadvantages of each technique [3, 17, 18].

5.3.3.1 O-15 Water

This tracer requires an on-site cyclotron and is often considered the ideal tracer for quantifying MBF in absolute terms. With no barrier effect from cellular membranes, the activity of O-15 water in an area of interest can be described by a one-compartment tracer kinetic model. Its use is limited due to a very short half-life (2 min) and poor contrast images between blood pool and the immediately adjacent myocardium [3, 6, 19].

Table 5.1 Advantages and disadvantages of SPECT and PET cardiac imaging

Advantages of SPECT	*Advantages of PET*
Widely available Standardized protocols Familiar procedure to healthcare providers Large evidence supporting efficacy and prognostic value	Superior image quality Higher diagnostic accuracy Lower radiation exposure Possibility of myocardial blood flow quantification (advantage in multivessel disease and microvascular disease) All studies done with attenuation correction
Disadvantages of SPECT	*Disadvantages of PET*
Higher radiation exposure Higher prevalence of equivocal studies Suboptimal identification of multivessel disease or balanced Unpredictable supply of Tc-99m tracers	Higher cost Limited availability for cardiac studies Less familiar to healthcare providers

5.3.3.2 N-13 Ammonia

N-13 ammonia is used to assess myocardial perfusion visually and with absolute quantification of MBF using dynamic acquisition from time of injection and a compartment kinetic model that incorporates extraction and rate constants. At physiologic pH, N-13 ammonia is in its cationic form and has a physical half-life of 10 min. The first-pass extraction is related to blood flow for low flow rates. It crosses myocardial cell membranes through passive diffusion or active transport. In the cell, N13 ammonia is incorporated into the amino acid pool as N13-glutamine or back diffuses into the blood. A 740 MBq (20 mCi) dose of N13 ammonia results in an effective dose of 1.48 mSv [3, 6, 19]. A typical imaging protocol for N-13 ammonia using regadenoson is shown in Fig. 5.5.

Typically 370–740 MBq (10–20 mCi) of N-13 ammonia is injected over 20–30 s. Dynamic images should be acquired immediately during infusion, and static images should be started 1.5–3 min after the end of infusion. Imaging duration is usually 10–15 min [3, 6].

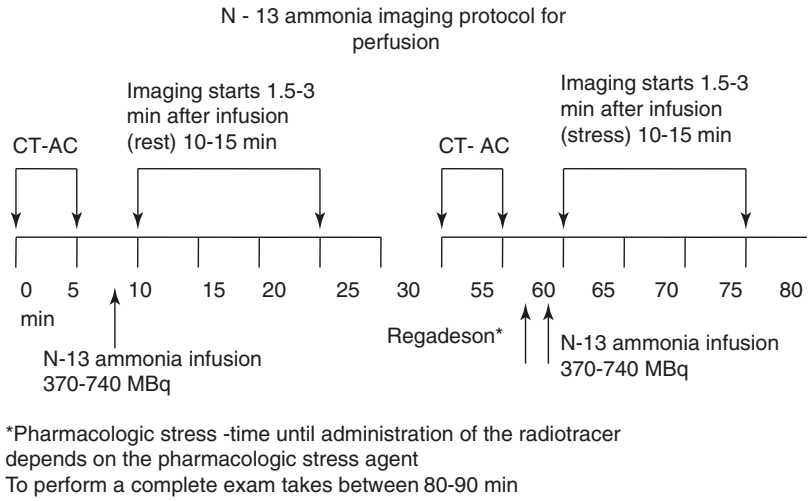

Fig. 5.5 N-13 ammonia rest and stress PET perfusion imaging protocol with regadenoson stress

5.3.3.3 Rubidium-82

Rb-82 is a monovalent cationic analog to potassium. It is produced by a generator system through decay from strontium-82 (Sr-82). It decays to rubidium-82, by emission of several high-energy positrons, and has a half-life of 75 s. It enters the myocyte via sodium/potassium adenosine triphosphate transporter. First-pass extraction is less than ammonia and decreases or plateaus with higher blood flow rates. The total effective dose for a maximal allowable activity of 2220 MBq (60 mCi) vary from 1.1 to 3.5 mSv [3, 6, 19]. A typical imaging protocol for Rb-82 rest and stress is shown in Fig. 5.6.

Perfusion imaging with Rb-82 can be acquired using 740–1850 MBq (20–50 mCi) of the tracer for each study with the type of detectors and acquisition parameters determining the exact dose. Rest images are acquired first to reduce contamination by stress effects. The tracer is infused during a maximum of 30 s and imaging started 70–90 s after injection if left ventricle ejection fraction is over 50% and 90–130 s if under that value [3].

Table 5.2 compares the differences between available SPECT and PET MPI tracers [18–20].

5.3.3.4 F-18 Flurpiridaz

This is a novel PET mitochondrial complex-1 inhibitor, structurally an analog to pyridaben. With the longer half-life of F-18 (120 min), there is no need for on-site cyclotron production. Image quality, compared with N-13 ammonia or Rb-82, is higher. Protocols can be performed with dynamic exercise or pharmacologic stress. A sustained higher extraction rate with high flow

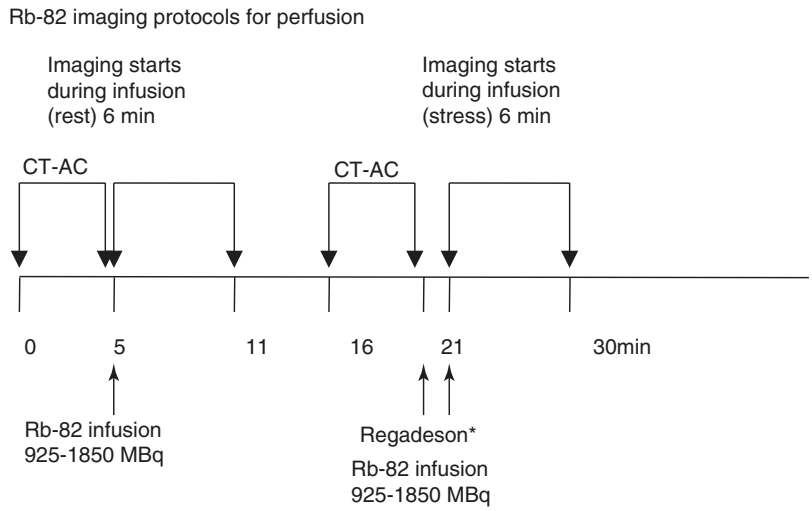

Fig. 5.6 Rb-82 rest and stress PET perfusion imaging protocol with regadenoson stress

Table 5.2 Comparison between the different perfusion tracers

Tracers	Production	$E_{\gamma\ rays}$ (KeV)	$T_{1/2}$	First-pass extraction, %	Inj. dose (MBq)	Total dose/study (mSv)
SPECT tracers						
^{99m}Tc	Generator	140	6 h	54–65	740–1480	3–16.3
^{201}Tl	Cyclotron	69–70	72 h	85	74–148	10.9–15.3
PET tracers						
^{15}O-H_2O	Cyclotron	511	2.06 min	100	No guidelines	No guidelines
^{13}N-NH_3	Cyclotron	511	9.96 min	80	370–740	1.5
^{82}Rb	Generator	511	1.25 min	65	370–2220	1.75–7.5

rates enables enhanced absolute quantification of blood flow. This tracer is not yet approved for clinical use [6, 19].

5.3.4 Pharmacologic Stress Agents and Protocols

All myocardial perfusion imaging studies should be performed using dynamic exercise stress whenever possible to obtain exercise duration, heart rate and blood pressure response, and variables that are important for CAD diagnosis and management and not available from pharmacologic stress [21]. Pharmacologic stress is reserved for patients who are unable to exercise, unable to achieve at least 85% of the maximal age-adjusted heart rate, or unable to reach an ischemic endpoint on the bases of symptoms or ECG changes. Sensitivity of MPI decreases in patients who achieve <85% of the predicted heart rate [22]. If the myocardial perfusion images are normal, it cannot be certain if they are truly normal or due to an inadequate level of stress achieved during submaximal exercise. Alternatively, if there is ischemia, it is never certain if the full extent of ischemia was detected.

The pharmacologic agents in common use include the vasodilators, adenosine, dipyridamole, and regadenoson, and the adrenergic stimulant dobutamine. The properties of these agents are shown in Table 5.3. The vasodilators produce maximal coronary hyperemia creating blood flow heterogeneity by causing a greater increase in

Table 5.3 Comparison between pharmacological stress agents

	Adenosine	Regadenoson	Dipyridamole	Dobutamine
Mechanism of action	Vasodilation through activation A_{2A} Also activates A_1 A_{2B} and A_3 receptors	A_{2A} adenosine receptor agonist	Prevents the intracellular reuptake and deamination of adenosine	Stimulation of b1 and b2 receptors (effect similar to exercise)
Increase in MBF	3.5–4	3.5–4	3.5–7	–
Peak effect	1–2 min	1–4 min	6.5 min	> 10 min
Half-life	10 s	First phase: 2–4 min Second phase: 30 min Third phase: 2 h	30–45 min	2 min
Administration	Continuous infusion 140 μg/kg/min over 4–6 min	Intravenous dose of 0.4 mg	0.56 mg/kg over 4 min	Given incrementally starting at 5–10 μg/kg/min, increasing every 3 min until 40 μg/kg/min or 85% of the predicted heart rate
Side effects	AV block, peripheral vasodilation and bronchospasm	Shortness of breath, headache, and flushing	Chest pain; headache; dizziness; extrasystoles; nausea; hypotension; flushing	Palpitation; chest pain; headache; flushing; dyspnea; supraventricular and ventricular arrhythmias
Absolute contraindications	COPD High-degree AV block or sinus node disease Hypotension or severe hypertension Unstable CAD Hypersensitivity to adenosine or regadenoson	COPD with ongoing wheezing High-degree AV block or sinus node disease Hypotension or severe hypertension Unstable CAD Hypersensitivity to adenosine or regadenoson	COPD Hypotension or severe hypertension Unstable CAD Hypersensitivity	Unstable CAD Hemodynamically significant left ventricular outflow tract obstruction Atrial tachyarrhythmias with uncontrolled ventricular response History of ventricular tachycardia Uncontrolled hypertension Aortic dissection Hypersensitivity

blood flow in territories perfused by normal coronary arteries and then in those perfused by arteries with flow-limiting stenosis. Dobutamine increases not only blood flow but heart rate and blood pressure, and this increase in myocardial work and oxygen demand may create true ischemia.

5.3.4.1 Vasodilators

Mechanism of Action, Safety, and Efficacy

Adenosine and regadenoson stimulate A_{2a} receptors directly producing coronary vasodilation. Adenosine is produced inside many cell types, and inside the cell, it has no effect on blood flow. It is actively transported into the extracellular space where it is capable of binding and stimulating a series of adenosine (A) receptors [23]. The A_{2a} receptors, present on vascular smooth muscle and endothelial cells, enhance arterial wall smooth muscle dilation and increase coronary blood flow. Adenosine also stimulates the A_1, A_{2b}, and A_3 receptors, which cause peripheral vasodilation, nonischemic cardiac chest pain, atrioventricular nodal block, and bronchospasm which are undesirable side effects in the context of perfusion imaging. Inactivation of extracellular adenosine, whether endogenously produced or exogenously administered, is under 10 s due to reuptake by all types of cells using the same cell membrane transport system and active metabolism [2].

Regadenoson is an A_{2a} agonist with a lower affinity for A_1 and almost no affinity to A_{2b} and A_3 adenosine receptors. The coronary vasodilatory effects are achieved during the first pass through the heart with a doubling of coronary blood flow by 30 s, and maximal plasma concentration is achieved in 2–4 min after injection. The loss of its pharmacodynamic effect on coronary blood flow occurs in approximately 30 min. The most common side effects of regadenoson are shortness of breath, headache, and flushing [2, 5].

Dipyridamole blocks the reuptake mechanism of adenosine and increases coronary blood flow by rising extracellular concentration of endogenously produced adenosine. Dipyridamole hyperemia lasts for more than 50 min, peak action occurs 6.5 min after the start of infusion, and the half-life is between 30 and 45 min [2].

Caffeine-containing beverages and foods and methylxanthine-containing medications, such as aminophylline, block adenosine receptors and thereby antagonize its effects; flow heterogeneity is not created with ingestion of these compounds and in patients with CAD; this may result in a false-negative test. This antagonist action, however, is helpful when side effects are present and administration of aminophylline blocks the adenosine receptors and reverses the side effects [2].

Side effects have been reported to occur in 50% of patients receiving dipyridamole with reversal required in 12%. Side effects occur in 80% of patients receiving adenosine with <1% receiving aminophylline reversal [24, 25]. Vasodilators cause, on average, a 10 mmHg decrease in systolic and diastolic blood pressure with a compensatory 12–15 beats per minute increase in heart rate [24]. The most common cardiac side effects with dipyridamole include chest pain (20%), ECG changes (16%), and ST depression (7.5%). With adenosine, the cardiac side effects included chest pain (35%), transient A-V nodal block (7.6%), and ST-T wave changes (5.7%). The majority of reported chest pain is not ischemic but due to nonselective stimulation of bradykinin pain receptors by adenosine. Patients with ECG changes consistent with ischemia are felt to have a higher dependence on collateral vessel blood flow which may be decreased due to coronary steal associated with a marked increase in coronary flow in normal vessels during vasodilation and a resultant decrease in collateral flow. At some institutions, it is standard practice to reverse the effects of dipyridamole in all patients using aminophylline. The effective half-life of dipyridamole is 30 min, which is longer than the half-life of aminophylline, and this means additional doses maybe required to prevent recurrence of side effects. Adenosine can be reversed by stopping the infusion. With regadenoson a lower incidence of chest pain, flushing, and throat, neck, and jaw pain are experienced, and a higher incidence of headache and gastrointestinal discomfort are reported. A rare but important side effect of regadenoson is an increase incidence of seizures. Patients having seizures associated with regadenoson use should not receive aminophylline for reversal as this has the potential to

increase seizure activity (see product package insert). Patients with unstable angina or decompensated COPD should not receive dipyridamole, adenosine, or regadenoson. As regadenoson is a more selective A_{2a} receptor agonist, it can be used in patients with mild to moderate asthma and moderate to severe COPD [2, 5].

Dipyridamole and adenosine have been used extensively and have an excellent overall safety record. More recently, regadenoson has also proved to have a good safety profile [26–28]. Although general side effects are common, cardiac and severe adverse events are rare. When considering that patients referred for pharmacologic stress testing are generally more debilitated, overall safety is comparable to that reported for conventional dynamic exercise stress testing [24]. Severe adverse complications such as death and myocardial infarction in association with pharmacologic stress testing are uncommon. In a retrospective review of 73,806 patients from 59 centers in 19 countries, there were 9 reported cardiac deaths and 13 nonfatal myocardial infarctions using intravenous dipyridamole [29]. In a prospective registry that included 9256 patients receiving intravenous adenosine, there were no deaths and one patient had a myocardial infarction [24]. The reported diagnostic accuracy using adenosine, regadenoson, or dipyridamole has been shown to be comparable to exercise. In early studies performed mostly using planar Tl-201 imaging in which each patient was studied twice with exercise and dipyridamole, sensitivity was in the 80% range and specificity in the range of 90%. There were no differences between the two forms of stress [30]. The published studies looking at the accuracy of adenosine stress did not in general perform stress twice and used predominately SPECT imaging with Tl-201 or the Tc-99m tracers. The average sensitivity for pharmacologic stress with vasodilators was 87%, and the specificity was 74% [30]. Regadenoson and adenosine were compared in the ADVANCE MPI trials, and regadenoson proved to induce similar perfusion defects as those observed with adenosine, irrespective to age, gender, diabetic status, body mass index, or prior cardiovascular history [26]. Based on extensive publications and practical clinical experience in everyday use, the accuracy of vasodilator pharmacologic stress is accepted as being equivalent to exercise stress.

Pharmacologic Stress Protocols

The vasodilator stress protocols using adenosine, dipyridamole, or regadenoson can be performed using low-level exercise stress prior to and during infusion to improve image quality, by decreasing background activity and lowering patient side effects. Figure 5.7 demonstrates the imaging protocol for adenosine pharmacologic stress.

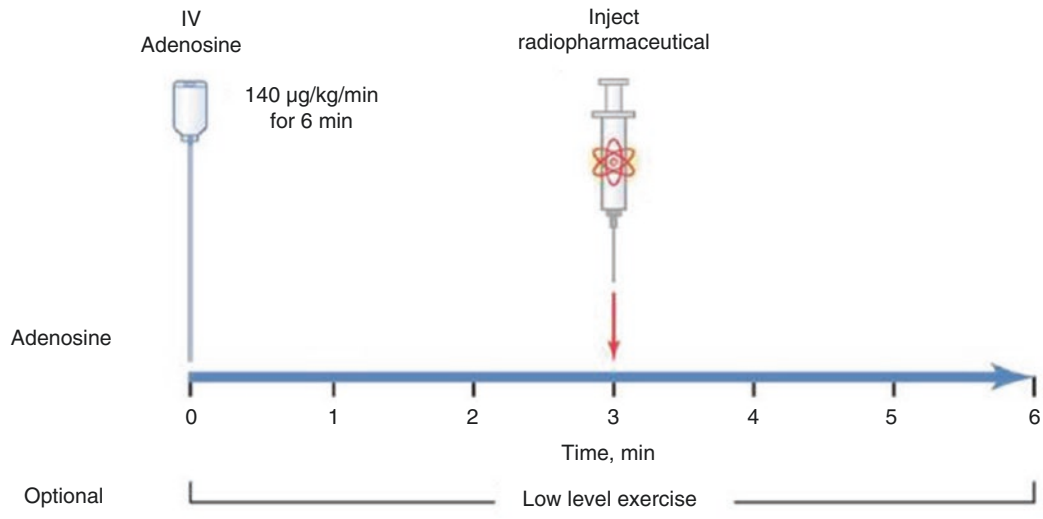

Fig. 5.7 Protocol for pharmacologic stress with adenosine

Patients should fast a minimum of 8 h and medications and foods containing caffeine stopped for 24 h. Methylxanthines and dipyridamole need to be stopped for 48 h prior to testing as they inhibit the vasodilatory effects of the adenosine and dipyridamole. Patients with 2° A-V nodal block (Mobitz Type II) or 3° A-V nodal block without a functioning pacemaker should not receive adenosine, regadenoson, or dipyridamole due to the potential A-V node blocking effects. Patients with a prolonged PR interval or Wenckebach can be tested safely. The use of vasodilator stress is recommended in all patients with a LBBB as the use of exercise leads to a higher rate of false-positive studies due to septal defects [31].

Adenosine is infused at a rate of 140 μg/kg/min for 4 or 6 min with the radiotracer injected at minutes 2 or 3 and the infusion continued a minimum of 1 min to allow maximal extraction, especially of the Tc-99m tracers which have a lower extraction fraction and then Tl-201 across the coronary bed. If the patient has evidence of ischemia by symptoms or profound ECG changes, the radiotracer can be administered earlier, but the infusion must be maintained a minimum of 1 min to allow radiotracer extraction at the high coronary blood flow rates. Performing low-level exercise during adenosine infusion decreases side effects and improves image quality and is recommended in all patients capable of walking on a treadmill [2].

Dipyridamole stress protocol is shown in Fig. 5.8. It is infused at a rate of 0.56 mg/kg of body weight over 4 min to a maximum total dose of 60 mg. Tl-201 or a Tc-99m radiotracer can be administered by bolus injection 3–5 min following completion of the infusion or earlier if the patient has evidence of ischemia by symptoms or profound ECG changes. Maximal coronary hyperemia is delayed due to the need to allow endogenous adenosine levels to increase following the inhibition of the adenosine reuptake mechanism by dipyridamole. Aminophylline administration is required more often due to the longer half-life, and side effects may recur due to the shorter half-life of aminophylline [2].

Unlike the other pharmacologic stress agents, regadenoson is given at a fixed dose of 0.4 mg, regardless of body weight, as a 10 s bolus. This is shown in Fig. 5.9. Since there is a very rapid increase in coronary blood flow, the radiotracer is administered 30 s after starting the regadenoson bolus [2, 5]. Since regadenoson is given as a bolus at a fixed dose, this allow it to be administered more efficiently to those patients who attempt dynamic exercise stress but are not able to achieve the target heart rate. In such patients, a bolus of regadenoson can be given while the patient is still on the treadmill or immediately in recovery. All the other stress agents require weight-based dosing and continuous infusion over several minutes to get the desired increase in

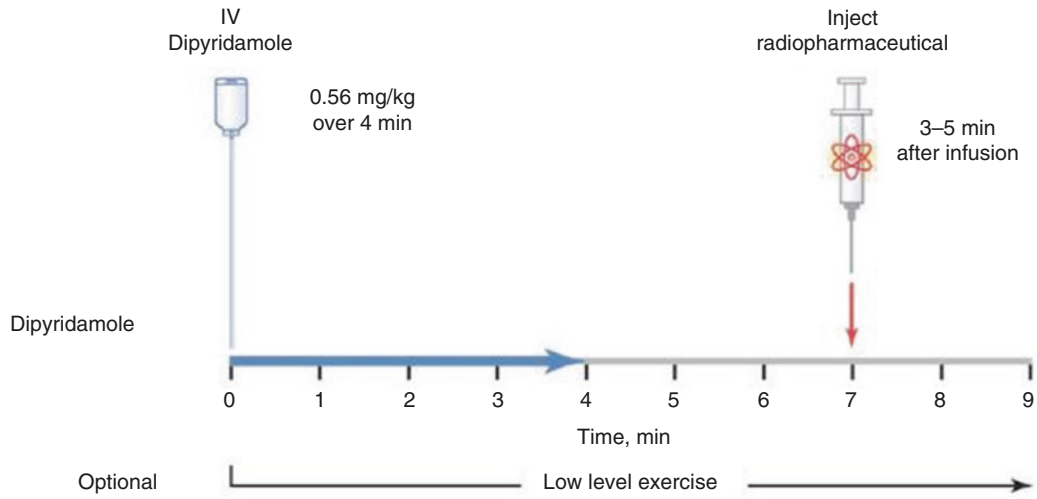

Fig. 5.8 Protocol for pharmacologic stress with dipyridamole

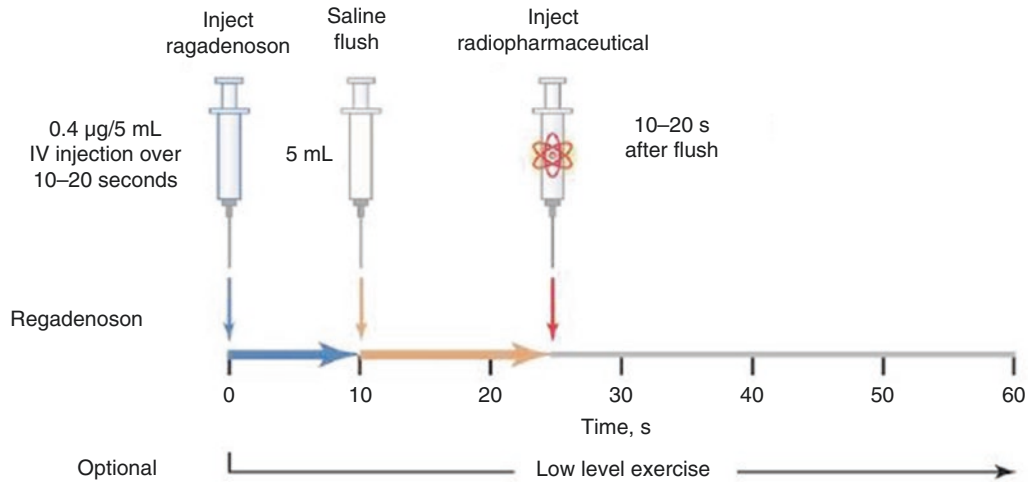

Fig. 5.9 Protocol for pharmacologic stress with regadenoson

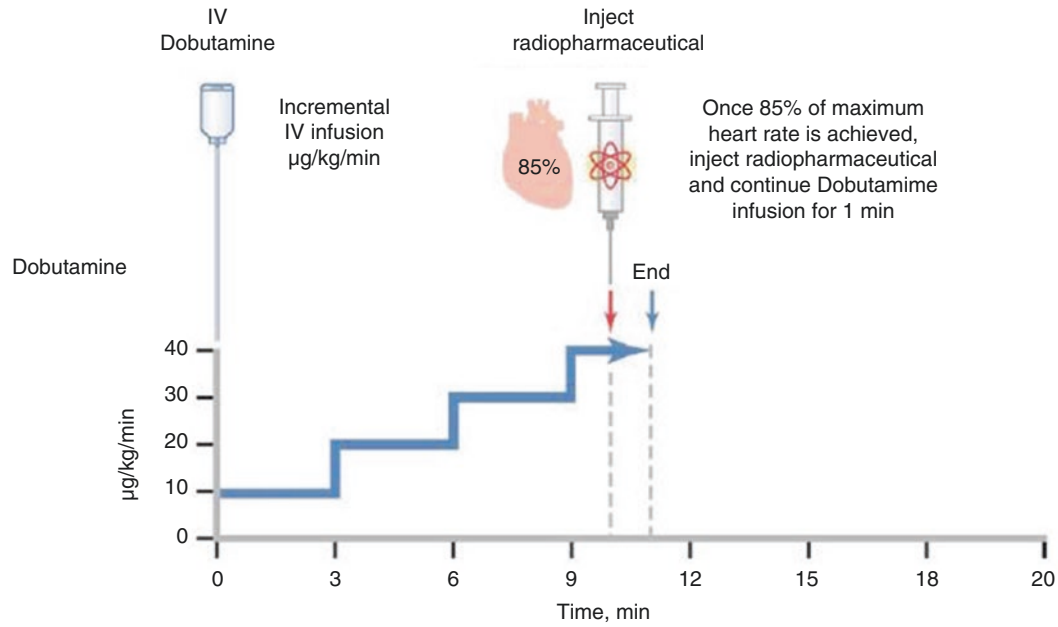

Fig. 5.10 Protocol for pharmacologic stress with dobutamine

coronary blood flow. This protocol has been shown to be safe but should not be used in patients who have achieved an ischemic endpoint even if they have not reached the target heart rate.

5.3.4.2 Catecholamines

Dobutamine is used infrequently for myocardial perfusion imaging. As shown in Fig. 5.10, the protocol requires 3 min stepwise infusion stages of increasing doses of dobutamine until an ischemic endpoint is reached or the patient achieves 85% of the maximal age-predicted heart rate. Protocols typically take much longer then vasodilator stress [32]. Patients with hypertension, abdominal aortic aneurysms, poorly controlled supraventricular arrhythmias, or ventricular arrhythmias should not be studied. Although some nuclear cardiology laboratories use it exclusively, at most centers it is used predominately in patients with severe and poorly con-

trolled lung disease and in patients who have ingested caffeine on the day of testing, and vasodilators cannot be used [2]. Studies with regadenoson have shown that it can be used safely in patients with chronic obstructive pulmonary disease or asthma.

5.3.5 SPECT and PET Image Acquisition

The recommendations for SPECT acquisition are summarized in Table 5.4 and for PET in Table 5.5.

Table 5.4 SPECT perfusion imaging with Tc-99m tracers

Patient position	Supine or prone to minimize diaphragmatic attenuation
Low-dose CT scan	
Gated CT scan	
Dosage	Higher dose is advised in the stress study, 890–1332 MBq (24–36 mCi); rest study, 296–444 MBq (8–12 mCi)
Route of administration	Intravenous
Delay time from injection to imaging	30–45 min
Delay time of the two sets of images	3–4 h
Energy window	140 KeV ± 15%
Collimators	Low-energy high-resolution (LEHR)
Orbit	180° from 45° RAO to 45° LPO (circular or noncircular)
Pixel size	6.4 ± 0.4 mm (64 × 64 matrix)
Acquisition type	Step-and-shot
Number of projections	64
Total time	Dependent on number of detectors but should get adequate number of counts in under 20 min to avoid patient motion
ECG gated	Standard in at least one of the acquisitions (stress)
Frames/cycle	8–16
Attenuation correction with CT	Optional

Table 5.5 PET-CT perfusion imaging

Radiopharmaceutical	^{82}Rb or ^{13}N-NH_3
Patient position	Supine, performed with a CT scout image or topogram
Low-dose CT scan	Slow rotation speed; high pitch; non-gated; acquired during tidal expiration breath-hold
Gated CT scan	Can be used for attenuation correction and calcium score quantification
Dosage[a]	^{82}Rb: 1.48–2.22 GBq for stress and rest images (40–60 mCi) ^{13}N-NH_3: rest images 0.37 GBq (10 mCi); stress images 1.11 GBq (30 mCi)
Route of administration	Intravenous
ECG gating image	For ^{82}Rb image begins 90–120 s after injection; for ^{13}N-NH_3 image begins 3–5 min after injection; the scan time is of 5 min for ^{82}Rb and 20 min for ^{13}N-NH_3
Dynamic imaging	Allows quantification of myocardial blood flow and for that purpose after injection imaging begins and continues for 7–8 min for ^{82}Rb or 20 min for ^{13}N-NH_3; to acquire dynamic and gated images, two separate injections of 82Rb are required; only one with ^{13}N-NH_3
List mode imaging	Ideal approach as a single injection allows multiple reconstructions but requires significant computer power
Stress	Pharmacological/exercise
Image reconstruction	Filtered back projection or iterative reconstruction
Attenuation correction	CT-based attenuation correction in almost all the cases; rotating rod sources

[a]3D imaging requires less dosage than 2D imaging

High-quality imaging and optimal diagnostic accuracy can be achieved through the selection of equipment and a well-designed quality assurance program.

The majority of SPECT systems are based on Anger camera technology where one or more camera heads rotate around the patient's body. Anger cameras consist of a collimator that selects photons traveling parallel to the collimator and a single NaI crystal that absorbs and amplifies incident gamma photons. The photomultiplier tubes (PMTs) further amplify the signal and spatially locate the scintillation events within the crystal.

New dedicated cardiac cameras are characterized by increased photon sensitivity. This is achieved by different collimator methods which include multiple pinhole collimators and ultrahigh-sensitivity detectors focusing on the heart. Sensitivity is also improved by the scanner geometry surrounding the patient. Solid detectors replace the combination of scintillation crystals with photomultiplier tubes, and this result in an improved energy resolution. These new scanners can reduce acquisition time or lower patient radiation exposure by allowing administration of a lower dose (Table 5.6) [33, 34].

Positrons are positively charged particles with the same mass as electrons. Annihilation occurs when a positron collides with an electron with the emission of two 511 KeV gamma rays, traveling in opposite directions. PET detectors fitted with various crystal materials are placed in a ring gantry surrounding the patient and configured to register only coincident photon pairs. Compared to SPECT, PET exhibits higher spatial and temporal resolution [3].

Table 5.6 Advantages and disadvantages of the cardiac dedicated ultrafast SPECT cameras

Advantages
Images may be acquired in reduced time without compromising quality
Images may be acquired with lower injected dose without compromising quality
More convenient for patients
The information provided has similar diagnostic quality
Disadvantages
Expensive
Limited availability
Lack of evidence due to their limited use

5.3.5.1 ECG Gating

Since being introduced in the early 1990s, it is now a critical element of all cardiac SPECT and PET studies [35]. ECG-gated perfusion studies allow the simultaneous acquisition of information regarding perfusion and global and regional left ventricular function and volumes. During gated acquisition, the ECG signal allows usually 8 or 16 intervals or time frames to be acquired for each beat with counts for each subsequent beat being added to the frames in the first beat. This is done for each beat in all the projections. The increasing number of frames gives higher count rates that allow more accurate assessment of the ejection fraction. Ejection fraction measured using 8 frames will give values that are approximately 3 ejection fraction units lower than when 16-frame acquisition is performed. Sixteen-frame acquisition allows analysis of filling and ejection rates that can be used for assessment of diastolic function [36].

For arrhythmia rejection, it is best to avoid selection of parameters that will compromise the perfusion information or prolong the acquisition. Thus, accepting all beats will guarantee high-count perfusion images without increasing the imaging time, but this may compromise the results of the ejection fraction calculation. To guarantee optimal perfusion information, a ±50% acceptance window around the pre-study sampled heart rate will give the most counts. Newer systems allow simultaneous and separate windows for static perfusion, keeping all beats, and ECG-gated windows, applying a narrower acceptance window. This allows getting the most accurate ejection fraction without compromising the perfusion data. Patients in atrial fibrillation with a narrow RR interval have accurate EF measurements. If more than one out of every six beats is an APC or PVC, EF measurements are not reliable. With increase in heart rate variability, the accuracy of the EF decreases. Review of the beat length histogram is advised as a quality control step for EF measurements.

Areas that have normal wall motion and thickening on the gated images may be associated with normal or ischemic myocardium. Apical thinning and areas with breast or diaphragm attenuation are also associated with normal wall motion. Since gated Tc-99m studies are acquired a minimum of 10–15 min following peak exercise stress, regional wall motion in most patients with ischemia usually returns to normal by the time of imaging. Severe ischemia induces persistent wall motion abnormalities that are detected during gated acquisition in as many as 1/3 of cases [10]. One of the most important benefits of gated SPECT acquisition is helping to differentiate attenuation due to the diaphragm or breast from areas of old myocardial infarction or scar [37]. Areas of scar have absent or diminished motion and thickening, while areas with decreased activity due to attenuation will show normal motion and thickening. Patients with prior heart surgery will show akinesis or hypokinesis of the septum because of the surgery in the absence of ischemia or infarction. Such areas will have normal thickening. Patients with LBBB or a paced rhythm will also demonstrate abnormal septal motion. In addition to improving diagnostic accuracy during subjective visual image interpretation, gated measurements of global ejection fraction and regional wall thickening have been validated using equilibrium blood pool imaging, cardiac catheterization, and cardiac MRI [38–41]. These studies found excellent agreement across EF values ranging from 12% to 88%. Small hearts gave very high EF values due to the poor spatial resolution of the SPECT systems.

The availability of automated methods for measuring ischemic or scar burden, LVEF, ventricular volumes, transient ischemic dilatation, and phase analysis have been attractive though, until now, underutilized [42]. The assessment of left ventricle mechanical dyssynchrony using phase analysis of gated SPECT or PET myocardial perfusion imaging has been shown to be related to the severity of heart failure and could potentially expand the indications of gated perfusion imaging. Compared with other techniques used for the same purpose, phase analysis offers simplicity and reproducibility. It can be applied retrospectively and combined with myocardial scar detection, and it can be used to optimize cardiac resynchronization therapy [43].

5.3.5.2 Attenuation Correction

Attenuation correction removes soft tissue artifacts from myocardial perfusion images. It can be performed using either a sealed source such as Gd-153 or an X-ray or CT-based method for acquiring the transmission maps. Gd-153 line source methods are only available on older systems. The size of the patient and the amount of tissue between the heart and the detector lead to attenuation artifacts that adversely affect image quality. Not only SPECT but also PET images are prone to attenuation due to the loss of true coincidence events either by absorption or scattering. All PET images are acquired with attenuation correction. It is well recognized that the ability to correct cardiac emission data for the effects of attenuation may improve significantly the interpretation of the reconstructed images [2, 5, 44].

5.3.5.3 Hybrid Imaging

Hybrid imaging combines different imaging modalities in a way where both contribute to the final information. Hybrid whole-body PET-CT and PET-MR in oncology allowed, for the first time, to associate anatomy with a functional radiopharmaceutical. Initially thoracic CT data was used only for attenuation correction of MPI, as mentioned above, but incorporating the information of the CT or MRI to SPECT or PET gives an additional input by providing morphology and functional assessment of the cardiovascular system [44–46]. Calcium scoring derived from these images may also prove useful for diagnosis and management.

5.3.6 Quality Control (QC) of the Images and Reporting

Once the SPECT or PET acquisition is completed, the results need to be reviewed to determine whether the patient can leave the laboratory or additional acquisition is required. Rotating projection images should be reviewed to unmask

potential sources of errors such as patient motion, low count density, extra cardiac activity, soft tissue uptake, or sources of attenuation. Processing can by performed by technologists or physicians but requires careful review by both the technologists before the patient leaves to see if re-imaging is required and the physician at the time of interpretation in order to see if technical factors will influence the perfusion images. Communication between the two is important in order to get the most accurate results. Orientation and segmentation should be in accordance with published guidelines [47]. Technical advances in computer processing are providing more options that should result in better image quality [2, 3, 5].

5.3.6.1 Quantitative Analysis of MPI

Visual analysis is the most common method of interpretation [47], but automated methods may be useful to provide over reads. For performing quantitative analysis, the limits for automated delimitation of the epicardial and endocardial borders should be manually defined and the generated images reviewed to make certain there is no tracking into hot areas outside the heart. Once the epicardial and endocardial borders and mitral valve plane have been visually verified, a polar plot is generated by comparison with a normal database. Polar maps reduce the three-dimensional information to a simple plot giving the severity and reversibility of perfusion abnormalities. All the above described steps are critical to get good results. Poor definition of the borders is likely to result in errors [48]. Sometimes the most difficult problem of using quantitative analysis is overcoming the fear of not calling abnormalities when they are identified as abnormal by the automated reading. This fear may be related to concerns about liability or an over eager need for high sensitivity to not miss any disease. In either case, it is important to reach a decision based on visual interpretation before reviewing the automated analysis. Some suggest that automated methods have a performance, if not superior, at least equivalent to visual scoring [49]. In fact they seem sensitive but less specific, and areas identified as abnormal by automated analysis are given a second look just in case something was missed. Problems with scaling, boundary definitions, inappropriate alignment, and scatter lead to erroneous quantitative results that should not lead to patients being inappropriately labeled as having CAD [50].

5.3.6.2 Absolute Quantification of Perfusion

Absolute quantification of myocardial blood flow is a potentially more objective and reliable analysis of the functional significance of a coronary stenosis. Although there are reports of such measurements using SPECT acquisition, PET remains the main method used to derive these measurements. It reduces false-negative results of perfusion due to balanced or subendocardial ischemia. Myocardial blood flow is measured in ml/min/g and assessed in hyperemic and rest conditions by dynamic acquisition with measurements of myocardial and blood pool time-activity curves. Absolute quantification potentially increases the value of PET perfusion imaging [3, 20, 51].

5.3.6.3 Image Interpretation

As mentioned above, accurate interpretation of MPI studies involves a systematic approach that starts with technical QC performed on the rotating projection images, rest/stress perfusion and function comparison, reaching a conclusion based on the imaging information, reviewing the clinical history and the stress test results, and reconciling all this data to reach a final conclusion. An important part of this process is the initial quality control that must be done on an interactive workstation that allows image manipulation and modification. The items mentioned in QC must be systematically examined on every study to identify technical factors that may influence the perfusion data seen on the aligned slices. False-positive SPECT MPI studies very often are due to poor-quality acquisition data that in the process of filtering, reconstruction, and display, perfusion defects are created and not recognized as artifact. Once this initial QC has been performed, the matched stress and rest slices must be aligned and reviewed ideally using at one or two color scales. The first one used should be

linear, preferably gray scale, which displays the data spectrum in a continuous manner. Color scales have different characteristics that require careful correlation with coronary angiography or patient outcomes to determine the accuracy of diagnosis for each individual laboratory.

5.3.6.4 Generating a Report

The final product of all the above steps is a report for the referring physician that includes an accurate, unambiguous, and clinically relevant assessment of the probability that the patient has abnormal myocardial blood flow. It is beyond the scope of this concise review to cover this most important detail [52–55]. Good communication is encouraged between the referring physician and the nuclear cardiologist not only to report the results but, even before the performance of the test, to discuss its appropriateness. In summary the report should contain information about the laboratory where the study is performed and details about patient demographics; the clinical indication should be stated; tracer administration protocol and image acquisition details are technical aspects that should be described; and finally the report of the findings should lead to a concise, unambiguous conclusion. Putting too many qualifiers in the conclusion negates the value of the test results for the referring clinicians.

5.3.7 Clinical Indications

5.3.7.1 Diagnosis and Risk Stratification of CAD

Sensitivity and specificity for MPI have been extensively reported; initially using planar Tl-201 to more recent publications using the Tc-99m tracers with SPECT, quantitative analysis, ECG gating, and PET [56, 57]. The accuracy is heavily influenced by the populations being studied and the type of stress and posttest referral bias. In a meta-analysis using primarily planar Tl-201 studies weighted by sample size, a sensitivity of 87% and a specificity of 64% were reported [58]. In an analysis including more contemporary studies with Tc-99m SPECT and gating, the sensitivity was found to be 87% and the specificity was 73% [1]. Tc-99m radiotracers provide the best quality gated images and are the most commonly used. PET has been compared with SPECT, and PET has a better diagnostic. In a meta-analysis with 11,862 patients, a sensitivity of 92.6% was achieved by PET compared to 88.3% with SPECT to diagnose CAD. No significant differences in specificity were reported [59]. Besides an improved accuracy to detect disease, PET allows the absolute quantification of myocardial blood flow which seems to unmask clinically significant CAD and offers an objective interpretation that is more reproducible than visual analysis. Quantitative PET measures when integrated with qualitative myocardial perfusion assessment provide superior diagnostic accuracy and improve the capacity to detect functionally significant coronary artery stenosis [60]. Despite the growing evidence that quantitative perfusion PET can play a major role in the clinical setting, there are not yet clear indications for its clinical use [61]. In addition PET exposes patients to lower radiation doses. Its limitations are mainly due to the high costs, cyclotron dependency when using N-13 ammonia or O-15 water, and limited availability of PET camera systems.

According to guidelines and appropriate use criteria, MPI is recommended when there is an intermediate pretest probability of disease or when risk stratification is mandatory after an established diagnosis [62, 63]. It is recommended that an exercise ECG test should be used first in a stepwise approach for patients with an intermediate risk for CAD who have a normal baseline ECG and are capable of performing dynamic exercise [64]. For patients who are unable to exercise, SPECT or PET MPI are capable of providing diagnostic and prognostic information that cannot be gotten from treadmill testing alone. However, such patients have more risk factors, and even if the perfusion study is normal, the occurrence of cardiac death is higher than in patients who are capable of exercising [65]. In patients who have positive ECG changes of ischemia, MPI provides additional information for management, especially in the intermediate risk

category [66]. In a study with 4649 intermediate Duke treadmill score patients who had normal perfusion, the 7-year cardiac mortality was very low at 1.5%, and the cumulative frequency of catheterization was 17% [67].

MPI is recommended in patients with abnormal ST segments, LBBB, ventricular paced rhythms, pre-excitation, LVH, or prior revascularization [64, 68]. The effects of referral bias, testing in patients with prior revascularization, and the documented occurrence of abnormal perfusion in patients without obstructive CAD but functionally abnormal flow reserve all influence the accuracy of testing when comparing it to the "gold standard" coronary angiography. For that reason, accuracy of testing for the detection of disease and assessment of prognosis will be discussed in the context of recognized specific patient populations that can influence the results of SPECT or PET testing.

5.3.7.2 Special Populations

Ethnic and Racial Differences

Most of the published data on SPECT is in Caucasian males capable of performing dynamic exercise. SPECT accuracy and prognosis results vary and usually loose accuracy and prognostic value when tests are performed in other groups [69, 70]. Many of these groups have a higher cardiovascular risk factor profile and other potential factors influencing test performance. African Americans have overall lower test accuracy and worse prognosis across the range of ischemia [70]. Whereas the death and MI rate in Caucasians is <1% with a normal SPECT MPI, two studies have shown it to be 2%/year in African Americans [69, 71].

Women

Ischemic heart disease is the leading cause of death in women in Western countries. The SPECT diagnostic and prognostic accuracy in women is influenced by gender differences in the prevalence of obstructive CAD and technical limitations due to breast attenuation and smaller left ventricular size. Low specificity was a major limitation in the early studies using planar Tl-201 that was overcome with the availability of SPECT and ECG gating and the use of attenuation correction. Using these techniques, gender differences in the performance of testing for diagnosis have been minimized, but not totally eliminated [72, 73]. It is known that the traditional approach to ischemic heart disease detection based on the identification of obstructive CAD is less effective when factors such as abnormal coronary reactivity, microvascular dysfunction, and plaque erosion with distal microembolization seemed to be related to chest pain in women. PET imaging could help to understand the mechanisms of CAD in women due to its ability to provide measures of blood flow and of coronary flow reserve [74–76].

Patients with LBBB/Pacemakers, Left Ventricular Hypertrophy, Nonspecific ST-T Wave Changes

For patients in these categories, treadmill testing does not provide accurate diagnostic or prognostic information, and SPECT MPI is indicated for evaluation. Patients with LBBB with exercise MPI have a low specificity in the LAD distribution due to a septal defect caused by diminished septal blood flow at high heart rates in the absence of obstructive CAD [77]. If there are associated defects in the apex or anterior wall, specificity is improved, but the use of vasodilator stress improves diagnostic accuracy and gives prognostic information. Overall prognosis is worse in such patients, but imaging is predictive of events. In 245 patients, the 3-year survival was 27% in high-risk scans and 87% in low-risk scans [77]. Less well documented is the effect of pacemakers on SPECT accuracy and prognosis, but such patients are treated in the same way as those with LBBB, and the prognostic value of SPECT is retained [78]. In the presence of LVH, hypertension, or nonspecific ST-T wave changes on the resting ECG, SPECT retains diagnostic and prognostic value [79, 80]. Well-trained athletes with LVH by echocardiography have been reported to have a higher incidence of false-positive studies due to "hot spot" scaling problems [81].

Asymptomatic Patients

Although testing is not recommended in asymptomatic patients, SPECT can detect the presence of disease and give prognostic information [82, 83]. Testing may be appropriate in high-risk occupations such as aviators, fireman, and policeman with multiple risk factors [64], but computed tomography coronary angiography with calcium score assessment seems to be the first approach for high-risk asymptomatic populations [63] .

Patients with Diabetes

Patients with diabetes are at a very high risk for having critical coronary stenosis and cardiovascular events [84]. Despite the diffuse nature of vessel involvement with a higher occurrence of balanced disease, SPECT has diagnostic and prognostic value [85–88]. In a retrospective analysis, event-free survival was found to be lower in diabetics across all categories of ischemia [87]. In a prospective study involving 1123 carefully screened asymptomatic diabetics, half were randomized to SPECT imaging, and 118 (22%) were found to have silent ischemia on SPECT of which 33 (6%) had moderate or large perfusion defects. The prevalence of silent ischemia was higher than expected. All patients in this study were prospectively followed to determine if the imaging results, which were not blinded, influenced management and long-term survival. It was found that among randomized patients, the event rates were low and not significantly reduced by perfusion imaging screening over 4.8 years. These results could reflect, partially, the impact of aggressive guideline-driven management of risk factors which improve outcomes regardless of the presence or absence of ischemia [89].

Patients with Chest Pain in ED

Patients presenting to an emergency department within several hours of chest pain and a nondiagnostic ECG and normal or equivocal troponins can be risk stratified based on acute injection at rest of a Tc-99m perfusion tracer [90]. Patients with a perfusion abnormality are at higher risk for having infarction or unstable angina and deserve very aggressive medical and interventional management. Such patients can have abnormal perfusion due to occlusion or spasm of an unstable vessel, and the perfusion abnormalities can be detected prior to elevation of serum enzyme markers [91–93]. The sensitivity of the procedure improves if the tracer administration occurs during or immediately after the chest pain episode. Studies performed in this context have shown a high-sensitivity and high-negative predictive value, and patients with a normal study who are discharged have a very low likelihood of having cardiac events. If the acute study is normal, it can be used as the resting image for comparison following exercise or pharmacologic stress to exclude underlying CAD in such patients. In a prospective randomized controlled study comparing resting SPECT imaging to conventional ED care, imaging significantly lowered hospitalization rates from 52% to 42% [93]. Several limitations are recognized to this approach, namely, the difficulty to distinguish a perfusion abnormality due to an old infarction from that due to an acute coronary syndrome and the availability of nuclear medicine laboratories working 24 h/day.

Patients Before and After Revascularization

Before revascularization, myocardial perfusion imaging either with SPECT or PET is used to assess the highly variable physiological relationship between coronary lesion severity and coronary flow reserve. Even in the presence of flow-limiting stenosis, if exercise or pharmacologic stress perfusion is normal or mildly abnormal, patients are at low risk for cardiac events [94]. Using SPECT as a gatekeeper for referral to coronary angiography has been shown to not only be cost-effective but in no circumstance does it place patients at a higher risk for cardiac death or nonfatal myocardial infarction in comparison to the more expensive and invasive approach of performing coronary angiography on all patients [95]. It also has a role in determining the sequence and number of grafted vessels in high-risk CABG patients and for identification of the culprit lesion at the time of PCI. According to the guidelines, in a symptomatic patient, an area of ischemia equal or above 10% is a recommendation to perform revascularization whenever possible [63].

In asymptomatic patients after percutaneous coronary intervention (PCI), routine myocardial perfusion imaging is not indicated at any time in the first 2 years following a procedure [96]. In the first few months after a procedure, it has been shown that <30% of symptomatic patients have documented stenosis [97]. In addition, periprocedural changes in the treated area may result in perfusion defects even in the absence of restenosis, and testing in the first 4–6 weeks following a procedure is not recommended due to the occurrence of false positives [98]. If ischemia is detected beyond the immediate period of the procedure, the prognostic value of SPECT persists, and the occurrence of cardiac death and MI is increased in patients with large amounts of ischemia [99]. With the placement of drug-eluting stents to prevent restenosis, delayed healing, prolonged inflammation, and exercise-induced paradoxical coronary vasoconstriction of the adjacent segment have been reported [100, 101].

Even with the altered anatomy following CABG, myocardial perfusion imaging retains diagnostic and prognostic accuracy early and late for detection of stenosis in grafts as well as progression in the native vessel [102–104]. Routine testing in asymptomatic patients is not recommended [96]. The extent and severity of perfusion abnormalities detected by SPECT is predictive of death in both symptomatic and asymptomatic patients in the first 5 years after surgical revascularization [104]. Beyond 5 years, it has been shown that the presence of ischemia is the strongest predictor of mortality [103, 105, 106]. In 9000 asymptomatic patients, the presence of ischemia predicted a 3% annual mortality [105].

Risk Assessment of Patients Before Noncardiac Surgery

Risk assessment prior to noncardiac surgery requires a thorough review of the clinical, demographic, and surgical indications of risk rather than nonselective use of MPI [107]. Major predictors of increased perioperative risk include recent acute MI, unstable angina pectoris, decompensated congestive heart failure, significant arrhythmias, high degree of atrioventricular block, and severe valvular heart disease. Such patients are already high risk, and SPECT is not indicated as it is unlikely to further stratify such high-risk patients [1, 108]. Perfusion markers of high risk include a large area of ischemia, perfusion defects in multiple vascular territories and transient left ventricular dilatation. The ACC/AHA guidelines recommend coronary angiography in patients in whom the results of the noninvasive testing indicate a high risk of cardiac events or in those with angina unresponsive to medical therapy. In low-risk patients with a low-risk surgery, myocardial perfusion imaging is not indicated [109]. In the last published ESC guidelines, MPI testing is advised before high-risk surgery in patients with two or more clinical risk factors and when functional capacity is poor (<4 Mets) and may be considered in those undergoing intermediate risk procedures [110].

5.4 Myocardial Viability

5.4.1 Basic Concepts

Viable myocardium refers to myocardial tissue that is still alive but hypokinetic due to persistent but low blood flow to living myocytes that decrease contractility to remain alive. This is the concept of hibernation initially identified by Rahimtoola [111]. The blood flow must be adequate to deliver enough glucose to maintain anaerobic glycolysis with a lower production of adenosine triphosphate (ATP) that is able to maintain transmembrane gradients and lactic acid washout but not enough to maintain contractility. Revascularization, by improving blood flow, would enhance oxygen delivery and beta-oxidation of fatty acids which allow a more efficient way of getting ATP and regain contractile function. Contractile dysfunction could also arise from a transient severe ischemia episode, with spontaneous recovery with time, called myocardial stunning. Although theoretically distinct, an overlap between the two could occur as repetitive episodes of ischemia, and stunning could lead to a state of chronic dysfunction and hibernation [112].

5.4.2 Nuclear Cardiology to Assess Viability

Viable myocardium could be identified by several techniques among which cardiac SPECT and PET have an important role.

SPECT is widely available and uses perfusion tracers such as Tl-201 or Tc-99m tracers to evaluate cellular integrity. Evaluation of viability with Tl-201 has been described in a previous section of this chapter. Resting uptake of Tl-201 or Tc-99m tracers is capable of identifying areas of myocardium that will show functional recovery after revascularization, but SPECT accuracy is best when a threshold of 60% of maximal myocardial tracer uptake is used for Tl-201 and 55% for the Tc-99m tracers [113]. There were no differences in predicting wall motion recovery between the three tracers using these thresholds.

PET is capable of evaluating metabolism either with a glucose analog, F18-fluorodeoxyglucose (F-18 FDG), or with C11-palmitic acid or C11-acetate. We will focus on F-18 FDG as it is the most used PET tracer for viability assessment. Areas of reduced resting myocardial perfusion and enhanced uptake of F-18 FDG are regarded as viable.

5.4.2.1 F18-Fluorodeoxyglucose (F-18 FDG)

F-18 FDG competes with glucose for transport and phosphorylation by hexokinase. As opposed to glucose, it doesn't proceed into glycogen synthesis and stays trapped in the tissue. It is a cyclotron-produced tracer with a half-life of 110 min. The administration of 10 mCi, intravenously, exposes to an effective dose of 7 mSv [3].

Viability Protocol

Figure 5.11 shows a frequently used protocol for viability assessment that can be used in both diabetic and nondiabetic patients. Myocardial perfusion at rest and stress or rest alone should be evaluated using Rb-82 or N-13 ammonia. The use of Tc-99m SPECT perfusion images for comparison to F-18 FDG PET should be discouraged due to the differences in image quality between the perfusion and metabolic images. For the F-18 FDG images, patient preparation is different whether identification of viability or inflammation is required. For viability, the goal is to enhance tracer uptake by the myocardium. Patients are fasted for at least 6 h; serum glucose is measured. A protocol of glucose loading and insulin is required (Fig. 5.11) prior to F-18 FDG administration. An initial glucose is measured, if

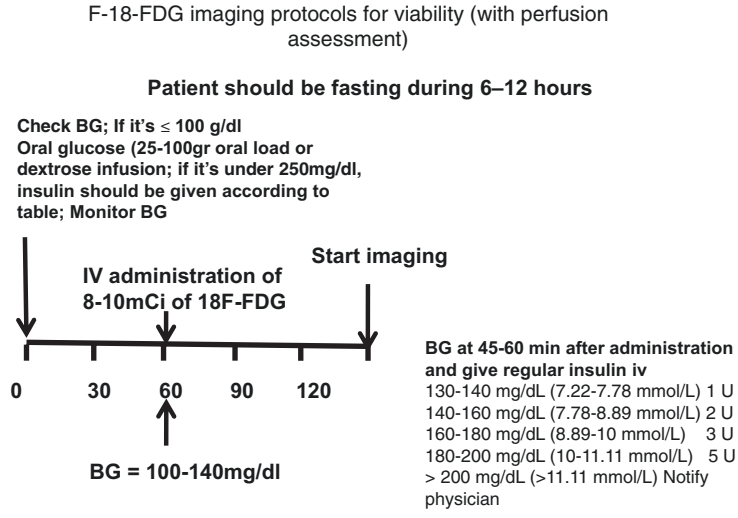

BG = blood glucose; FDG = fluorodeoxyglucose; IV = intravenous; mg = milligram; mmol = millimoles;L = liter; dL = deciliter; U = unit

Fig. 5.11 F-18 FDG imaging protocol for viability assessment

<100 mg/dl 25–100 g oral load or dextrose infusion is administered. When the initial glucose is ≤250 mg/dl, insulin is administered in the units shown in Fig. 5.11. Patients with glucose values >250 mg/cl should be canceled and a better preparation implemented. Diabetic patients are challenging due to their limited ability to produce or respond to insulin stimulation [3].

In a viability study, myocardial areas that have a perfusion/metabolism mismatch, consisting of severely diminished or absent perfusion but preserved or enhanced metabolic activity, have a high probability of regaining function after revascularization, and are hibernating but viable. Fig. 5.12 is an example of a rest/stress Rb-82 perfusion and F-18 FDG study showing myocardial ischemia and viability in three views. The stress images on the top row show extensive areas of abnormal perfusion involving the anterior, lateral, inferolateral, and inferior walls. The rest images in the middle row show marked improvement in the apical, midcavity, and basal areas, but they are not completely normal. There is enhanced right ventricular uptake in an enlarged and hypertrophied right ventricle on stress as well as dilation of the left ventricle with transient ischemia dilation (TID) giving a ratio of 1.27. On the F-18 FDG images, bottom row, there is enhanced FDG uptake throughout the anterior, lateral, inferolateral, and inferior walls. In this situation there was enhanced F-18 FDG uptake in areas with decreased perfusion identifying areas of hibernation. The areas that were ischemic have enhanced FDG uptake on the basis of memory of ischemia whereby the transient ischemic areas switched from fatty acids to the use of FDG. Only the basal anterior wall had diminished uptake on stress, rest, and FDG indicating that this areas was scarred.

5.4.3 Clinical Indications

5.4.3.1 Ischemic Cardiomyopathy

The presence of viable myocardium favors revascularization in the management of ischemic heart failure. Several observational studies seemed to support this notion, but until now prospective studies designed with this purpose failed to prove completely the concept [114]. The benefits of

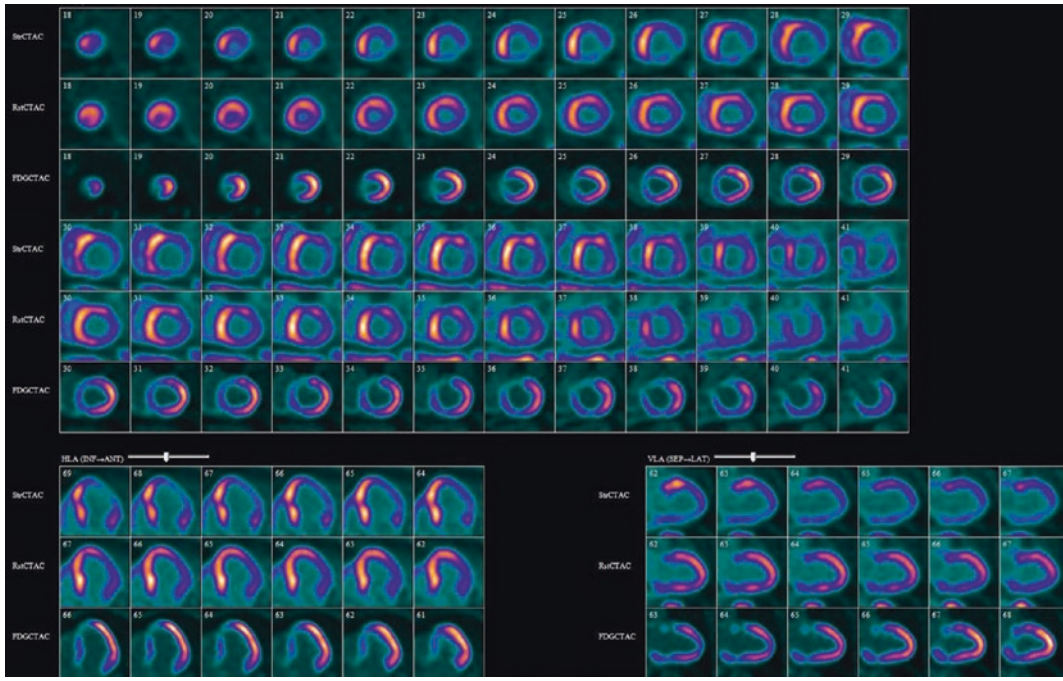

Fig. 5.12 Rest and stress Rb-82 perfusion and F-18 FDG viability PET study showing extensive ischemia and viability in the anterior and lateral walls

revascularization in terms of survival and symptoms seemed to be positively related to the amount of viable tissue and inversely related to the extension of scar [115–119]. Detection of myocardial viability is still a matter of debate, and more evidence is necessary to emphasize its role in the management of ischemic heart failure.

5.5 Assessment of Ventricular Function by Radionuclide Ventriculography

Assessment of ventricular function and volumes is essential to risk stratify cardiac disease. Equilibrium radionuclide angiography (ERNA) and first-pass radionuclide angiography (FPRNA) are reliable and robust methods to assess ventricular function. In the past, they were used widely but have declined due to the use of methods, such as echocardiography and cardiac MRI, that could provide more extensive information without radiation exposure and with ECG-gated SPECT MPI. These factors in combination with the declining availability of small field view cameras, that are optimal for high-quality studies, have resulted in resting ERNA studies being performed almost exclusively for monitoring chemotherapy-induced cardiotoxicity and heart failure. It is not likely that the use of these techniques will increase in the future.

5.5.1 Equilibrium Radionuclide Angiocardiography (ERNA)

The nomenclature for this technique includes MUGA (name of an early software program) and equilibrium-gated blood pool imaging and radionuclide ventriculography. It can be used to determine global and regional left ventricular (LV) and right ventricular (RV) function at rest and following exercise or pharmacologic stress. Analysis of the time activity curve provides information on systolic and diastolic function. Both planar and tomographic methods have been used for acquisition, but planar predominates due to ease of use and extensive experience [120].

5.5.1.1 Technique

Radiopharmaceuticals and Red Blood Cell Labeling

The basic technique uses stannous pyrophosphate to create a favorable oxidation/reduction environment inside red blood cells (RBC) so that when 10–30 min after Tc-99m pertechnetate is administered, it binds to hemoglobin and remains attached. Labeling can be accomplished in three ways: in vivo, modified in vivo/in vitro, and in vitro. There are differences in the efficiency of labeling, defined as the percentage of total radioactivity attached to RBCs versus the time and expense required to perform the technique. The amount of the stannous agent required for optimal labeling is in the range of 0.03–0.15 mg/ml of blood or 10–20 mg/kg of body weight. The usual administered activity is 800 MBq (23 mCi) for adult patients. The effective dose is of 5.6 mSv.

Labeling Techniques

In Vivo: This is the simplest, fastest, and least expensive labeling method but gives the lowest labeling efficiency. The stannous pyrophosphate is given intravenously followed 15 min later by Tc-99m which can be given as a rapid bolus for first-pass radionuclide angiography (FPRNA). This method achieves only 80–90% RBC labeling and the background activity is higher due to labeling of structures outside the vascular space such as the stomach and thyroid.

Modified In Vivo/In Vitro: The stannous pyrophosphate is given intravenously, and 20–30 min later, an aliquot of blood is withdrawn into a syringe containing the Tc-99m pertechnetate, and this is gently shaken for 10 min before being injected back into the patient. The labeling efficiency approaches 95%.

In Vitro: This should be performed under strictly aseptic conditions, in a laminar airflow unit dedicated to cell labeling. An aliquot of blood is withdrawn and centrifuged and the RBC pellet washed and incubated first with stannous pyrophosphate followed by the Tc-99m before being reinjected into the patient. There are commercial kits available which give a labeling efficiency of >97% [120].

Instrumentation and Procedure

Rest studies allow longer acquisition times and can be performed with a high-resolution collimator (parallel hole or slant hole). A collimator with 30° angulation allows optimal separation of the left atrium from the LV especially in patients with a horizontally positioned heart. Stress studies are limited to a 2 min acquisition at rest and peak stress, and in such situations a low energy all-purpose collimator gives a higher count rate. Cameras should be peaked at 140 ± 10 keV. The heart rate is sampled prior to acquisition to establish the time interval for each frame, and a ±10–15% arrhythmia rejection window should be used with elimination of the early beat as well as the next beat which has a longer filling period. List mode acquisition allows 10 ms temporal resolution and maximal flexibility in image processing but is memory intensive, and many of the current programs do not make it easy to acquire or process studies. Buffered beat techniques with forward and backward reconstruction of the time activity curve to eliminate drop-off in counts provide greater flexibility when diastolic function analysis is required. In order to measure the minimum volume in the time activity curve at end systole, a minimum of 16 frames is required to get an accurate ejection fraction (EF) in patients with fast heart rates or rest or during exercise stress. Rest studies with very slow heart rates require up to 32 frames to get accurate EF measurements.

Acquisition can be set up based on acquiring a fixed number of beats, time, or counts. Whichever method is used, it is necessary to acquire a minimum of 20,000 cm^{-1} over the center of the LV to get sufficient information density for an accurate EF calculation. The patient is positioned, and three views are acquired. The most important view for calculating the EF is the left anterior oblique (LAO) which provides the best septal separation between the two ventricles. Once this view has been acquired, the camera head is rotated 45° in the anterior direction and 45° toward the left lateral to get orthogonal views [120]. An example of the three acquired views at end systole and end diastole is shown in Fig. 5.13.

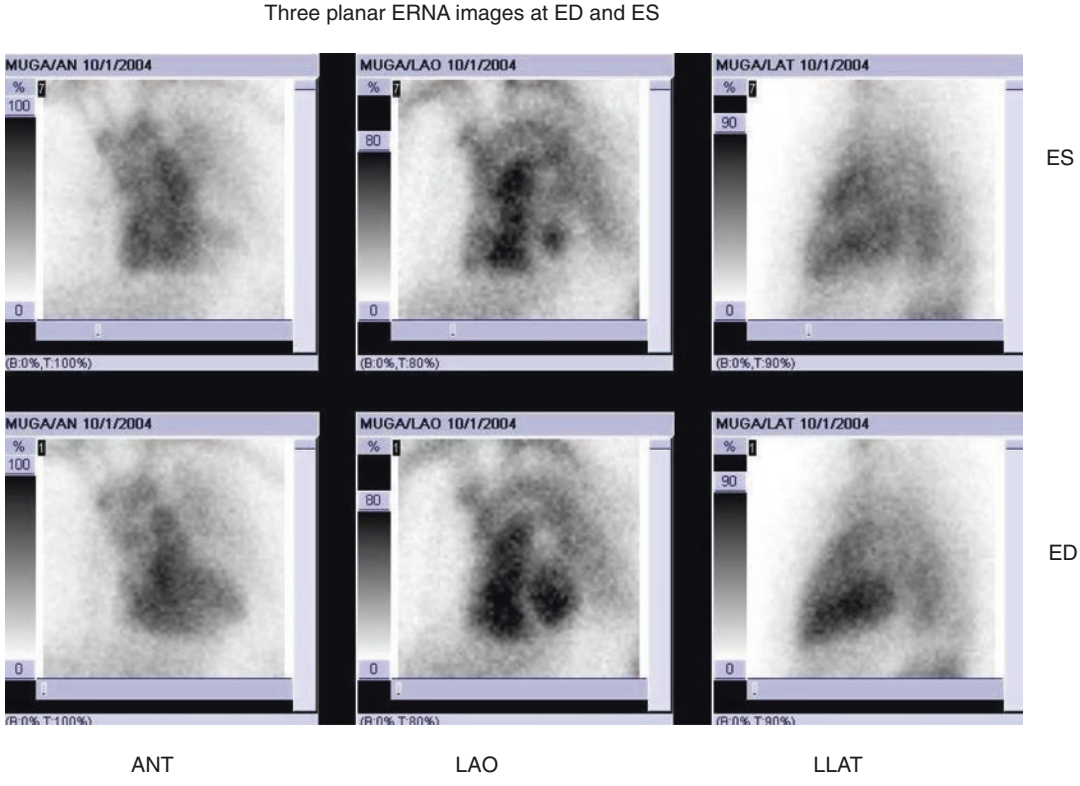

Fig. 5.13 Three planar ERNA views at end systole and end diastole

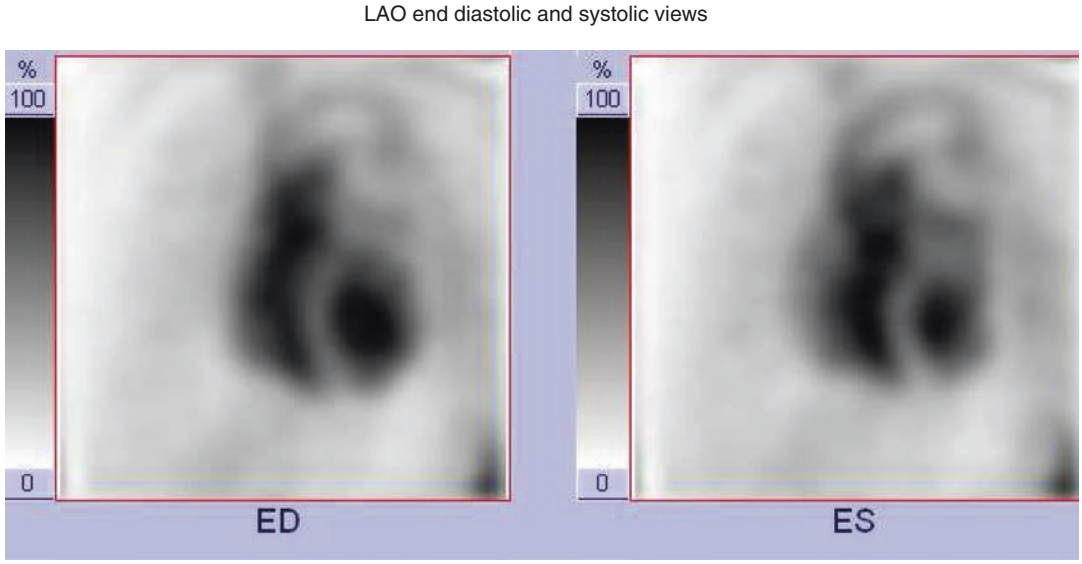

Fig. 5.14 ERNA LAO views at end diastole and end systole

Once acquisition is completed, the images are temporally and spatially smoothed, and three views in a cine loop should be reviewed in gray scale for a visual assessment of global and regional function to correlate with the quantitative EF. The beat-length histogram should be reviewed for adequacy of ECG gating.

Figure 5.14 shows how the septum separates the LV from surrounding structures at ED and ES in the LAO view. Calculation of the EF requires measuring counts or volume from the LAO view in the isolated LV at end diastole (ED) and end systole (ES) after correcting for the background activity as shown in Fig. 5.15. The left atrium can be seen popping up behind the LV on the ES frame. Background correction is necessary to eliminate the effects of blood pool activity in the structures overlaying and adjacent to the LV that do not change cyclically as in the LV function during its contraction. This background region is placed in the LAO view adjacent to the heart anywhere from 2 to 5 o'clock with care to avoid the left atrium, descending thoracic aorta, gastric, or spleen free

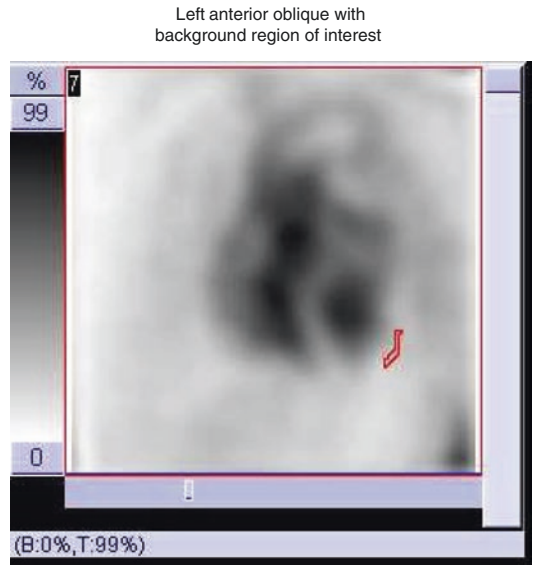

Fig. 5.15 LAO view with background region of interest

Tc-99m pertechnetate uptake. Putting the background area in any of these regions will lead to erroneous results. To estimate the EF, the following formula is currently used.

$$\text{LVEF} = \left[\left(\frac{\text{Background Corrected ED counts} - \text{Background Corrected ES counts}}{\text{Background Corrected ED counts}}\right)\right] \times 100.$$

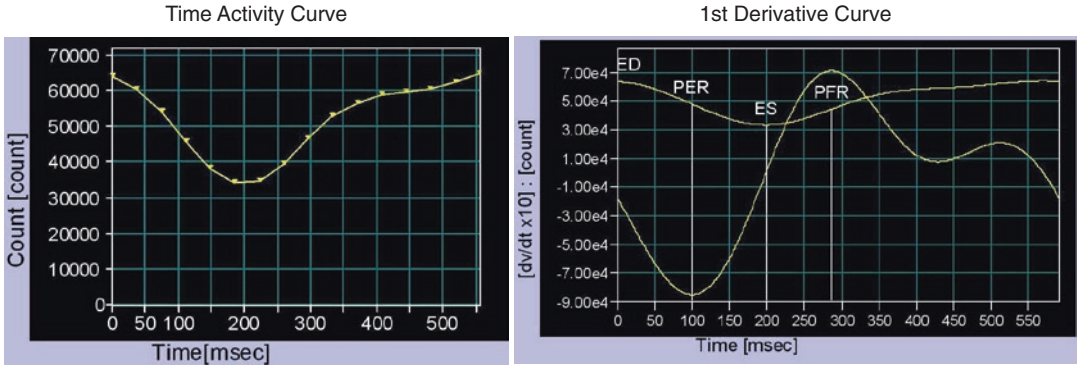

Fig. 5.16 Time activity curve and first derivative curve on LAO ERNA

Analysis of systolic and diastolic function using emptying and filling rates can be performed on the time activity curves as shown in Fig. 5.16.

Exercise Studies

To detect CAD, dynamic exercise can be performed using upright or supine bicycle exercise following RBC labeling. The patient is positioned on the bicycle with the camera in the LAO position, and a 2 min acquisition is performed for a baseline measurement. Incremental exercise is performed in 3 min stages during which the patient exercise for 1 min before a 2 min acquisition until the patient reaches symptom limited maximal exercise. In patients without CAD or other forms of heart disease, with peak exercise there is a minimum augmentation in global EF by at least 5 EF units from the baseline measurement. In patients with critical flow-limiting stenosis, EF may drop, stay the same, or fail to augment by at least 5 EF units. Attempts to look at regional wall motion rather than the global EF response to improve sensitivity have not been successful due to the limited regional wall motion assessment available from the single LAO planar view.

5.5.1.2 Clinical Indications

Assessment of LV Function

ERNA is capable of providing accurate and consistent measurements of LV global and regional function. Although RV EF can be measured, overlap of the right atrium does not allow complete isolation of counts or volume in the RV, and this introduces errors depending on the position of the two chambers. Assessment of diastolic and systolic filling and emptying rates requires accurate time activity curves for analysis which conventional frame mode acquisition does not provide [120].

Detection of CAD

With the availability of SPECT MPI, this technique is not used widely. Since the EF response to exercise may be abnormal in patients with nonischemic cardiomyopathies and other forms of cardiac muscle disease, specificity was low. In a composite of the published literature, a sensitivity of 86% and a specificity of 79% have been reported [121]. For patients unable to exercise, vasodilator stress does not provide sufficient accuracy in the ability to induce global or regional functional changes.

Monitoring Cardiotoxicity

ERNA continues to have a role in the serial monitoring of adults receiving anthracyclines or trastuzumab for the treatment of cancer [122]. This approach allows patients to receive the highest possible doses of these drugs for effective tumor treatment at the lowest possible risk of developing cardiotoxicity which in early studies could be as deadly as the tumor being treated. A baseline EF is measured prior to treatment. If normal, monitoring should be performed when doses of 250–300 mg/m^2 are achieved and then repeat the assessment at 450 mg/m^2 and afterward before every treat-

ment. If the EF drops ≥10% and reaches values below 50%, consider therapy discontinuation. If the EF is less than 50%, treatment could proceed with EF evaluations before each session, and a EF drop of ≥10% (EF units) or an EF ≤ 30% therapy discontinuation should be considered. If the EF is ≤30% at baseline, alternative methods should be used [123]. According to the position paper published by the ESC, ERNA can be used for monitoring cardiotoxicity. Since there are several cardiac imaging modalities available, the choice depends on local availability and expertise. The same modality should be used throughout the treatment. In this setting, ERNA has the great advantage of reproducibility, but radiation exposure and limited structural and functional information on cardiac structures should be considered [124]. Attempts to develop less toxic drugs or to pretreat patients with agents to lower or prevent cardiotoxicity have been under development, and serial monitoring is still required [125, 126].

5.5.2 First-Pass Radionuclide Angiography (FPRNA)

FPRNA can be used to assess left and right ventricular function at rest or during stress. It provides information on wall motion, ejection fraction, and assessment of systolic and diastolic parameters. It is best performed with a dedicated multicrystal or digital system, capable of delivering a minimum of 150,000 counts/s, to provide sufficient information density. A bolus of radioactivity is injected into the venous system, and multiple serial images are acquired at a 25–100 ms frame rate that allows the radioactivity to be tracked from when it enters the RV to when it exits from the LV. Using individual or summed time frames, measurements of global and regional RV and LV function can be performed. If there are atrial or ventricular shunts present, these may be detected and measured. Despite these unique features, the lack of adequate equipment, and payer reimbursement for performing studies, it is seldom performed in current clinical practice.

5.5.2.1 Instrumentation and Procedure

Studies are best performed using Tc-99m DTPA as the radiopharmaceutical which is cleared by the kidneys which is sufficiently far from the heart to not cause interference in case a second bolus injection is required. The injection site should be in a large vein to allow rapid, compact bolus administration. Injection rate should be slower if RV function is required or more rapid if LV function or shunt detection are the issues. Patients are positioned upright or supine in the anterior or a shallow RAO position for rest or exercise studies. The choice of collimators and the window time frame depends on what is the main purpose of the study. For patients performing exercise, motion correction methods should be used [120].

5.6 Neurocardiac Imaging

5.6.1 Basic Concepts of Neurocardiac Imaging

Cardiac autonomic control depends on the circulating neurotransmitters, norepinephrine and acetylcholine, and local innervation by the sympathetic and parasympathetic systems.

Myocardial sympathetic fibers are relatively abundant in the ventricles, especially in the left ventricular anterior and lateral walls. They run adjacent to the coronary arteries, in the epicardium, before penetrating into the myocardium. Central nervous system control of the sympathetic output depends on signals by the brain itself or by peripheral receptors. The descending pathway involves the spinal cord and the paravertebral stellate ganglia.

There are few parasympathetic fibers in the heart, especially in the ventricles. They are involved in the innervation of the atria and the inferior wall of the left ventricle, and they also modulate the atrioventricular nodal function. They begin in the medulla and run along the vagus nerves.

Norepinephrine is produced in the presynaptic terminal, stored in vesicles, and released in

response to a stimulus into the synaptic space where it binds to postsynaptic receptors. The sympathetic response depends on two processes: norepinephrine transport I uptake, which is the most important regulator, that controls the uptake, storage, and/or the catabolic disposal of norepinephrine, and the uptake 2 referring to the nonneuronal postsynaptic uptake of the neurotransmitter.

SPECT and PET autonomic radiotracers were first used to detect adrenal neoplasms. I123-metaiodobenzylguanidine (MIBG) is a physiologic analog of guanidine. It shares the transport pathway of norepinephrine and accumulates and displaces the neurotransmitter from the storage granules. Besides the use of I123-MIBG with SPECT, other radiotracers are used to assess myocardial sympathetic innervation. PET tracers, such as C11-hydroxyephedrine or C11-ephedrine, more similar to noradrenaline, with better image properties due to their higher uptake 1 selectivity, have been used. Their clinical application is limited by the short half-life of C11 [2, 3].

5.6.2 Imaging Myocardium Sympathetic Innervation

I-123-MIBG emits 159 KeV photons and has a half-life of 13.2 h. Radiation exposure after an administered dose of 370 MBq (10 mCi) is 5 mSv with the highest exposure in the bladder, liver, spleen, gall bladder, heart, and adrenals [2, 5].

Imaging, as shown in Fig. 5.17, is performed at rest and requires discontinuation of medications and substances known to interfere with the mechanisms of noradrenaline uptake (opioids, cocaine, tricyclic antidepressants, sympathicomimetics, antipsychotics, and some antihypertensive drugs). Prior to administration of I-123 MIBG, iodine may be given to block uptake by the thyroid. Intravenous administration of 370 MBq (10 mCi) over 1–2 min followed by saline flush is usually performed with the patient already positioned under the camera. Planar imaging is performed at 15 min and 4 h with SPECT imaging optional at 4 h. A standard Anger gamma camera with a low-energy high-resolution collimator is used, and almost all the published work used data from planar imaging. The use of a medium-energy collimator may result in better image quality. Analysis of the anterior planar image is used to calculate the ratio between heart and mediastinum uptake of the tracer, heart/mediastinum ratio (H/M), and in the difference of tracer uptake and retention in early and late images – washout rate (WR). Regions of interest (ROI) are drawn around the heart and in the mediastinum, and values of H/M from 1.9 to 2.8 are considered normal. Four examples are shown in Fig. 5.18 with the anterior images on the left column and the regions for the ratios on the right for a range of ratios. With the highest ratio, the

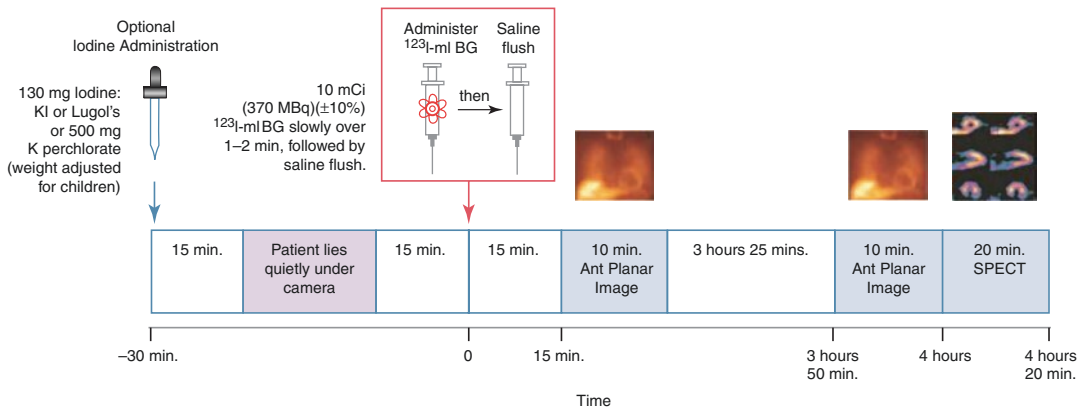

Fig. 5.17 Imaging protocol for I-123 mIBG cardiac imaging

heart can be visualized with uptake, but with the lowest ratio, the heart is barely visible and the lung up is markedly increased. For the WR a formula is used considering the uptake in early and late images [2].

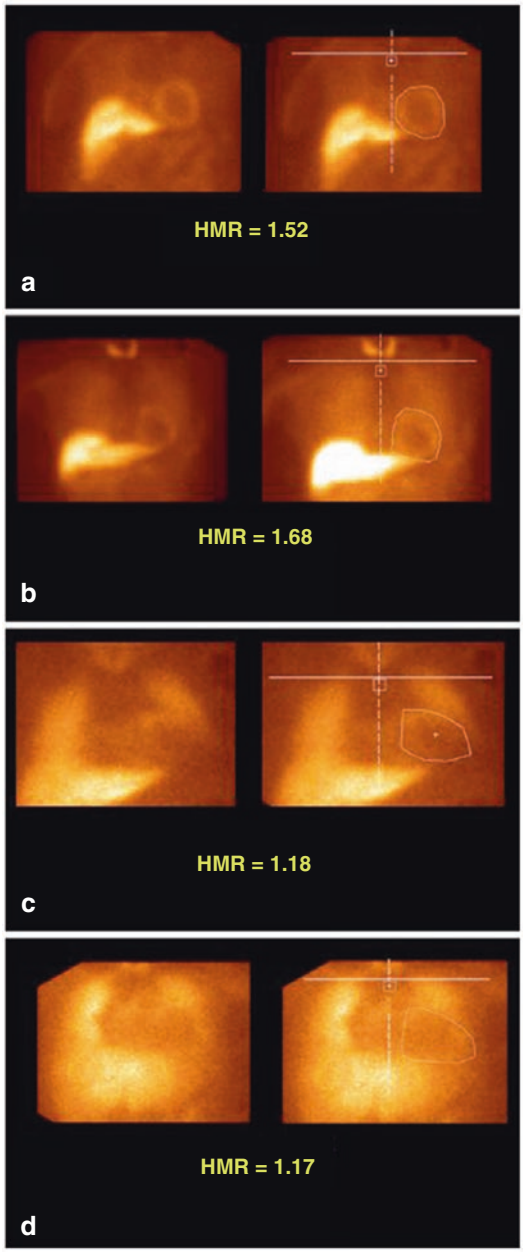

Fig. 5.18 Examples of I-123 mIBG anterior planar imaging in a variety of myocardial innervation

5.6.3 Clinical Indications

5.6.3.1 Heart Failure

The most investigated use of I-123 MIBG sympathetic imaging is in heart failure. In fact this condition involves disruption of the neurohumoral equilibrium, activating the renin-angiotensin-aldosterone system and the sympathetic system. In the initial stages of the disease, there is an increased response of the SNS in patients with low cardiac output which leads to increased norepinephrine release and transport. Eventually there is downregulation of the postsynaptic receptor number. With disease progression, the NET 1 transport system becomes overwhelmed leading to downregulation and spillover of the norepinephrine resulting in an increased washout ratio of MIBG. Presynaptic function decreases with time due to a loss of neurons and downregulation transport, and this leads to decreased cardiac uptake in advanced disease (low H/M ratio).

Several observational studies related the uptake of MIBG with the prognosis of heart failure with decreased ejection fraction [127]. The AdreView Myocardial Imaging for Risk Evaluation in Heart Failure (ADMIRE-HF) trial was a prospective, multicenter international study enrolling 961 patients with an ejection fraction equal or below 35% and in NYHA class II–III. The results showed that during the 17 months of follow-up, an H/M $\leq$ 1.6 was related to worsening NYHA class, life-threatening arrhythmias, resuscitated cardiac arrest, appropriate implantable cardioverter defibrillator discharge, and cardiac death of all causes. In a sub-analysis of the ADMIRE-HF, it was found that the H/M ratio added significantly to the prognostic power of the Seattle Heart Failure Model that incorporated all the patient clinical variable into the model [128].

5.6.3.2 Ischemic Heart Disease

Sympathetic innervation plays an important role in ischemic heart disease. Sympathetic fibers are more sensitive to ischemia than myocytes, so in myocardial infarction, the area of sympathetic

denervation is more extensive than the infarct area. The PAREPET trial (Prediction of ARrhythmic Events with Positron Emission Tomography) examined the utility of autonomic, perfusion, and viability imaging in patients with ischemia cardiomyopathy (NYHA I–III and LVEF ≤35%). Perfusion images were obtained with N13 ammonia, and viability was identified by F-18 FDG and innervation with C11-HED. In a 4-year follow-up, the occurrence of sudden cardiac arrest increased in relation to the severity and extent of C-HED autonomic image abnormalities [129]. Autonomic nervous system imaging has a promising role in heart failure.

5.7 Nuclear Techniques in the Management of Inflammatory, Infectious, and Infiltrative Heart Diseases

Nuclear cardiology techniques have an increasing and important role in management of systemic inflammatory diseases involving the heart. Inflammatory diseases such as sarcoidosis and infiltrative disease such as amyloidosis are among those where radiotracer techniques can contribute to an early diagnosis and monitor therapeutic approaches [130, 131].

5.7.1 Sarcoidosis

Sarcoidosis is a systemic granulomatous disease, where cardiac involvement is a major cause of death. In patients with systemic sarcoidosis, cardiac involvement is present in approximately 25–30%. Typical presentations of cardiac involvement include heart block, ventricular arrhythmias, myocardial thickening, diastolic dysfunction, fibrosis, dilatation, and systolic dysfunction [130].

Early detection is important in order to make therapeutic decisions such as aggressive anti-inflammatory therapy, implantation of a cardioverter-defibrillator, and eventual heart transplantation in some patients [132, 133]. There may also be a role for serial monitoring of the response to therapy, but at this time there is insufficient data to know the true role this will play in the future.

The inflammatory nature of sarcoidosis leads to a potential role for PET perfusion and F-18 FDG imaging as granulomas have increased metabolic activity due to increased use of glucose by inflammatory cells. There may also be a noncoronary distribution interference in myocardial blood flow due to arterial compression and dilation as well as eventual myocardial scaring. The major limitation of F-18 FDG is the nonspecificity of glucose uptake. Normal myocardium derives a portion of its energy production through glucose even though there is a preference for the use of fatty acids. Thus, the suppression of myocyte glucose uptake is critical to improving the specificity of FDG PET imaging. Despite these limitations, the use of PET is superior to other nuclear techniques such as SPECT with gallium-67 [134].

A typical protocol for the F-18 FDG PET evaluation of cardiac sarcoid is shown in Fig. 5.19. The best patient preparation involves a 24–48 h diet low in carbohydrates and sugar and high in protein and fat. In addition to this diet, patients should fast for a minimum of 12–18 h. The use of low-dose intravenous unfractionated heparin, 50 IU/kg, is recommended. Heparin causes the liver to release fatty acids that become available as myocardial substrate and thus decrease glucose utilization by myocytes. Diabetics present unique problems, and the recommendations are to use a high fat/low carbohydrate diet and hold oral medications the morning of the study. Diabetics on insulin should hold their long-acting insulin for 48 h and fast-acting insulin the morning of the examination. Getting dietary compliance is difficult, and there is no way to adequately monitor compliance.

It is recommended that whole-body imaging be performed, or at a minimum the chest, to look

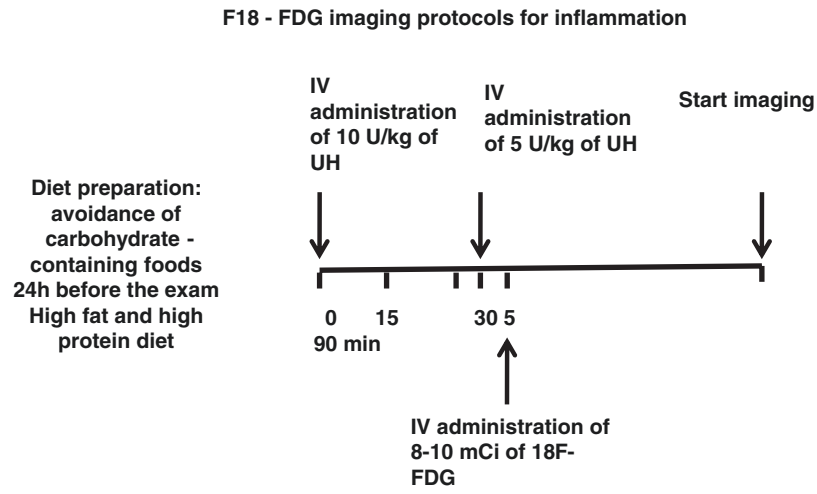

Fig. 5.19 Patient preparation and F-18 FDG imaging for myocardial inflammation

for noncardiac sarcoid involvement. Visual image interpretation is performed looking at reoriented serial slices in three views and comparing the resting perfusion Rb-82 or N-13 ammonia to F-18 FDG. This means that the images are normalized individually for the perfusion and FDG which is not optimal for interpretation as very low myocardial uptake when normalized may display images of homogenous or focal uptake. For this reason, it is recommended that quantitative measures such as standardized uptake values (SUVs) be used to avoid the issues associated with normalization.

Figure 5.20 shows serial resting Rb-82 perfusion and F-18 FDG slices in three views. On the perfusion images, there is a septal perfusion defect extending from the apical to basal slices, and the remainder of the myocardium has normal perfusion. On the FDG images, there is enhanced FGD uptake in the lateral wall starting at the apex and extending all the way to the base and involving the adjacent anterior and inferior walls. Although the basal lateral wall, especially when adjacent to a papillary muscle with marked uptake, can be a normal variant, the extent of the uptake observed is greater than would be expected as a variant. Since this patient does not have coronary artery disease, the perfusion defect in the septum is most consistent with scarring of the septum.

Although PET perfusion/metabolism imaging in patients with suspected or known sarcoid is promising, the lack of specificity for glucose uptake is a major problem that will need to be overcome by developing granuloma-specific tracers. Even with the continued use of FDG for inflammation, quantitative methods of analysis are needed.

5.7.2 Amyloidosis

Amyloidosis encompasses a broad spectrum of diseases that have in common the multisystem deposition of insoluble fibrillary proteins, known as amyloid fibrils, which ultimately lead to increased local oxidative stress, mechanical disruption, and tissue damage. Cardiac amyloidosis involvement is recognized but is probably underdiagnosed.

All types of amyloid are characterized by extracellular deposition of misfolded genetically abnormal or genetically normal transthyretin or light chain proteins manufactured in the bone marrow or liver. Several forms of cardiac involvement have been identified with important differences in diagnosis, prognosis, and treatment. Defined by their precursor proteins, the common types are:

1. Amyloid light chain (AL), due to deposition of immunoglobulin light chains, which is the most aggressive form, and where cardiac involvement, present in 50% of the cases, shortens life

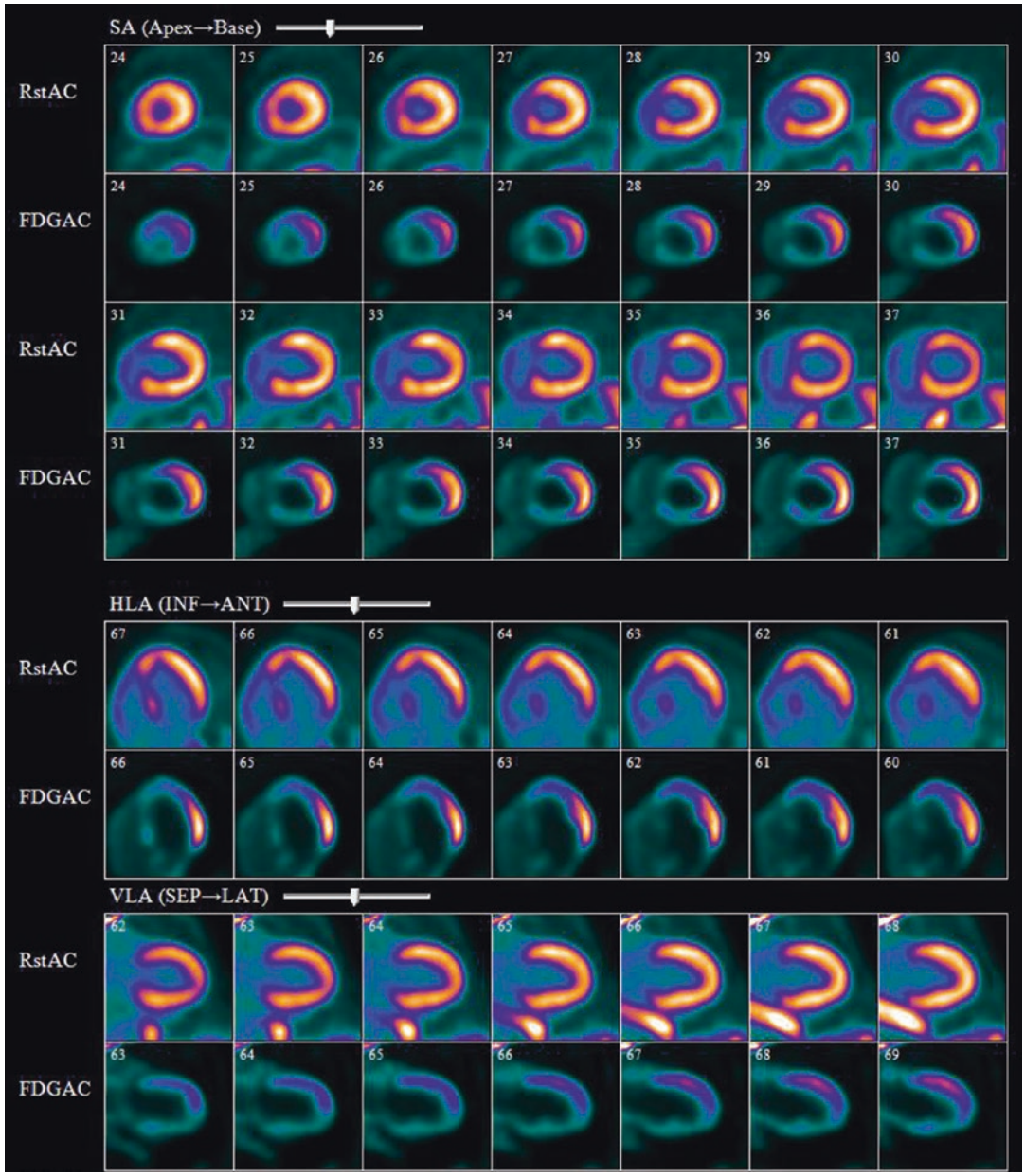

Fig. 5.20 Example of Rb-82 perfusion and active inflammation using F-18 FDG in suspected sarcoid

expectancy significantly. Frequently seen in patients with multiple myeloma.

2. Hereditary transthyretin-derived amyloidosis (ATTRm), an autosomal dominant disease, caused by more than 80 mutations of the protein transthyretin with a significant involvement of the peripheral nervous system and the myocardium.
3. Wild-type or senile transthyretin (ATTRwt). Probably the most common form and estimated to be present in 5–18% of patients over age 65 with heart failure with preserved EF. High prevalence in patients with aortic stenosis.

ATTR is also used to define presence of transthyretin amyloid without designation of

wild or mutant type. The extracellular deposition of amyloid fibrils leads to abnormalities in cardiac contractility, conduction, and perfusion. Patients develop symptoms of a restrictive cardiomyopathy. The involvement of the conduction system leads to various degrees of atrioventricular node block and ventricular arrhythmias. Microvascular disease is also common, giving rise to ischemia [130].

The final diagnosis is based on several procedures that culminate with endomyocardial biopsy as it is crucial in the identification of the specific type of amyloidosis for management. Given the invasive nature of myocardial biopsy and the need for immunohistochemistry or mass spectroscopy in inconclusive cases, readily available imaging techniques have been sought. With the pending approval of several drugs for treatment, the diagnosis is needed to select patients who will benefit. Echocardiography and cardiac MR have evolving roles.

Radioisotope imaging techniques, initially developed for detection of remote infarcts or bone imaging, identify the presence of transthyretin deposits in the myocardium. The two most commonly used radiotracers are Tc 99m-DPD (diphosphonate), available in Europe, or Tc 99m PYP (pyrophosphate) used exclusively in the United States. Studies using I123-MIBG have also performed to characterize the involvement of the peripheral nervous system of the heart by the ATTRm [135].

5.7.2.1 Imaging Protocols for Transthyretin Cardiac Amyloidosis

Imaging Procedures: There is no specific patient preparation required prior to the study. Patients are injected with 370–740 MBq (10–20 mCi) of Tc99m PYP or DPD. A variable period of time is required to get the tracer out of the blood pool and into the bone and myocardium. A 1-h wait is the most convenient for patients but is limited by persistent blood pool activity and mild uptake in bone. A 3-h delay allows blood pool clearance and higher concentration in the myocardium and bone but is inconvenient for patients. There is no consensus on which of the two time points is optimal for imaging. Both planar and SPECT supine images of the chest to include the heart and adjacent lung fields are acquired using small or large field of view cameras. When using small field of view cameras, it is essential to make certain that the contralateral lung filed is in the field of view to calculate a ratio. Whole-body imaging to look at other boney structures is optional but recommended.

Image Interpretation: Both the planar and SPECT images need to be reviewed for visual semiquantitative and quantitative interpretation. Depending on whether images are acquired at 1 or 3 h postinjection, there may be differences in visual scoring and quantitative analysis. Visual interpretation involves scoring the activity in the myocardium relative to bone uptake using the following system: Grade 0, no myocardial uptake and normal bone uptake; Grade 1, myocardial uptake <rib uptake; Grade 2, myocardial uptake equal to rib uptake; and Grade 3, myocardial uptake >rib uptake. At 3 h on planar or SPECT, a score ≥ 2 is considered positive for transthyretin amyloid.

Quantitative analysis can be performed on the planar anterior image using a region of interest that includes the myocardium but excludes the ribs and sternum. The total counts in the heart (H) are calculated. This same region should be moved to the contralateral lung field (CL), again being careful to avoid the sternum and ribs. The counts in the heart should be divided by the counts in the contralateral lung to get the H/CL ratio. When imaging at 1 h, a H/CL ratio ≥ 1.5 is considered ATTR positive and ratios <1.5 as ATTR negative. For 3-h images, a ratio ≥ 1.25 is considered ATTR positive and ratios <1.15 as ATTR negative.

Figure 5.21 is an anterior Tc-99m PYP whole-body image at 3 h in an 85-year-old male with severe dyspnea that worsens when he goes into atrial fibrillation. He had recurring right pleural effusions, and on echocardiography his EF is 60%. The image shows diffuse, marked uptake in the left chest with a H/CL ratio of 2.1. Also seen

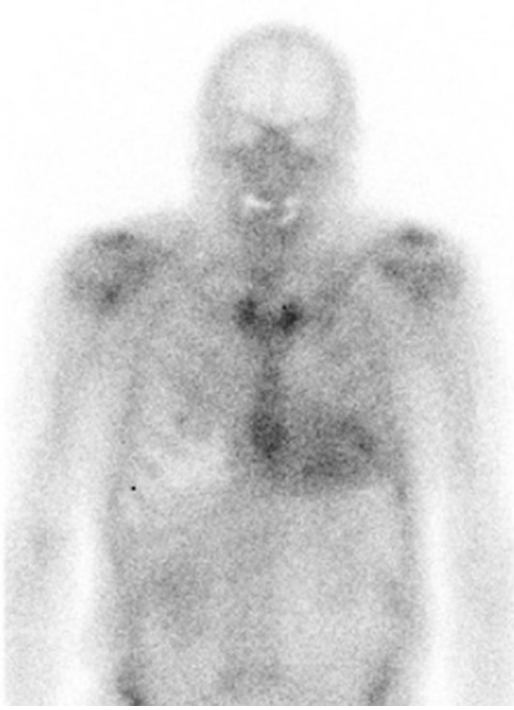

Fig. 5.21 Anterior Tc-99m pyrophosphate amyloid scan at 3 h in a patient with heart failure and preserved ejection fraction showing diffuse myocardial uptake in the heart

is a low count area in the right lung field corresponding to an existing pleural effusion. Fig. 5.22 shows serial slices in three views on the reoriented SPECT images in the same patient. There is very homogenous amyloid uptake throughout the myocardium that looks almost like a perfusion study.

5.7.3 Myocardial Infections and Endocarditis

Radionuclide techniques using both SPECT and PET may be used for diagnosis of infections in the heart caused by endocarditis, abscess formation, or infected devices such as pacemaker leads. Currently F-18 FDG PET imaging has the greatest interest and utilization but is limited by uptake in normal myocardium that requires aggressive measures to suppress normal uptake in order to differentiate between areas of normal myocardium and pathologic inflammation. Agents that specifically target components of inflammation are needed but not widely available.

The diagnosis of endocarditis using the Duke modified criteria is suboptimal in general and even lower when prosthetic materials such as heart valves and pacer/defibrillator leads are present. Echocardiography has a pivotal role in the management of this condition, but other imaging modalities have been used with good results. Cardiac computed tomography and magnetic resonance imaging are excellent in providing high-quality anatomical information. Radionuclide techniques provide physical/functional information that is increasingly important in the diagnoses and therapy monitoring of the disease.

The guidelines of the ESC include the use of nuclear techniques, namely, PET-CT with F-18 FDG and SPECT with Tc 99m-HMPAO (hexamethylpropyleneamine oxime)-labeled leucocytes in specific conditions of endocarditis [136]. A statement from the AHA mentioned the use of other imaging techniques, namely, PET-CT with FDG, although more data is required to define accuracy. Enhanced metabolism due to inflammation results in FDG uptake, and leucocytes are recruited to sites of active inflammation [137]. As was mentioned for the diagnosis of sarcoid with F-18 FDG, myocytes also take up FDG so meticulous patient preparation to suppress myocyte FDG uptake is required to improve specificity.

The advantages of using these imaging techniques are due to the ability to provide excellent functional information as opposed to just anatomic findings which can be nonspecific, especially in the postoperative setting. Both techniques demonstrated added diagnostic value in difficult cases involving prosthetic material (prosthetic valves, pacemakers, implantable cardioverter defibrillators, or ventricular assist devices) as well as demonstrating extracardiac foci of the disease [138].

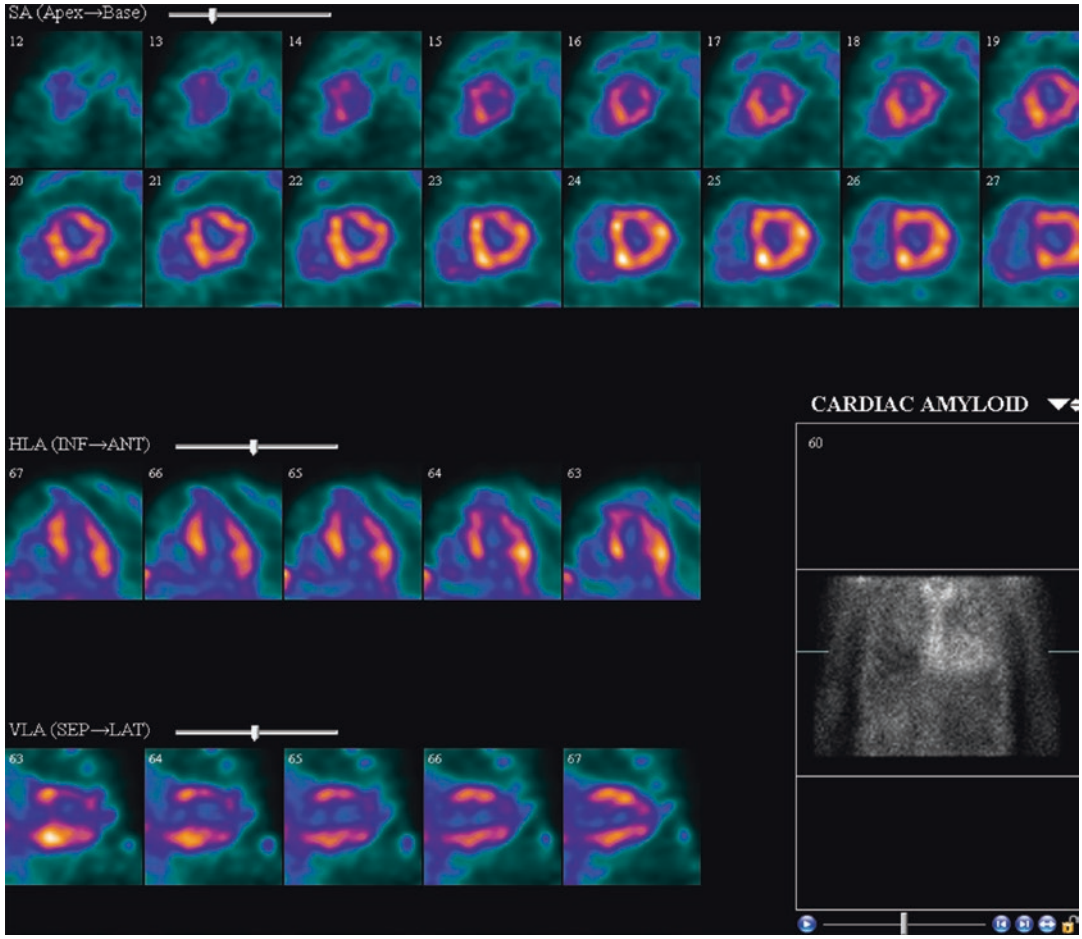

Fig. 5.22 Serial three-view Tc-99m pyrophosphate amyloid scan and anterior projection showing very homogenous uptake in the myocardium

References

1. Klocke FJ, Baird MG, Lorell BH, Bateman TM, Messer JV, Berman DS, et al. ACC/AHA/ASNC guidelines for the clinical use of cardiac radionuclide imaging--executive summary: a report of the American College of Cardiology/American Heart Association Task Force on practice guidelines (ACC/AHA/ASNC Committee to revise the 1995 guidelines for the clinical use of cardiac radionuclide imaging). J Am Coll Cardiol. 2003;42(7):1318–33.
2. Henzlova MJ, Duvall WL, Einstein AJ, Travin MI, Verberne HJ. ASNC imaging guidelines for SPECT nuclear cardiology procedures: stress, protocols, and tracers. J Nucl Cardiol. 2016;23(3):606–39.
3. Dilsizian V, Bacharach SL, Beanlands RS, Bergmann SR, Delbeke D, Dorbala S, et al. ASNC imaging guidelines/SNMMI procedure standard for positron emission tomography (PET) nuclear cardiology procedures. J Nucl Cardiol. 2016;23(5):1187–226.
4. Schelbert HR. Anatomy and physiology of coronary blood flow. J Nucl Cardiol. 2010;17(4):545–54.
5. Verberne HJ, Acampa W, Anagnostopoulos C, Ballinger J, Bengel F, De Bondt P, et al. EANM procedural guidelines for radionuclide myocardial perfusion imaging with SPECT and SPECT/CT: 2015 revision. Eur J Nucl Med Mol Imaging. 2015;42(12):1929–40.
6. Sogbein OO, Pelletier-Galarneau M, Schindler TH, Wei L, Wells RG, Ruddy TD. New SPECT and PET radiopharmaceuticals for imaging cardiovascular disease. Biomed Res Int. 2014;2014:942960.
7. Udelson JE, Bonow RO, Dilsizian V. The historical and conceptual evolution of radionuclide assessment of myocardial viability. J Nucl Cardiol. 2004;11(3):318–34.

8. Camici PG, Prasad SK, Rimoldi OE. Stunning, hibernation, and assessment of myocardial viability. Circulation. 2008;117(1):103–14.
9. Thompson RC, Heller GV, Johnson LL, Case JA, Cullom SJ, Garcia EV, et al. Value of attenuation correction on ECG-gated SPECT myocardial perfusion imaging related to body mass index. J Nucl Cardiol. 2005;12(2):195–202.
10. Johnson LL, Verdesca SA, Aude WY, Xavier RC, Nott LT, Campanella MW, et al. Postischemic stunning can affect left ventricular ejection fraction and regional wall motion on post-stress gated sestamibi tomograms. J Am Coll Cardiol. 1997;30(7):1641–8.
11. Sharir T, Germano G, Kang X, Lewin HC, Miranda R, Cohen I, et al. Prediction of myocardial infarction versus cardiac death by gated myocardial perfusion SPECT: risk stratification by the amount of stress-induced ischemia and the poststress ejection fraction. J Nucl Med. 2001;42(6):831–7.
12. Mathur S, Heller GV, Bateman TM, Ruffin R, Yekta A, Katten D, et al. Clinical value of stress-only Tc-99m SPECT imaging: importance of attenuation correction. J Nucl Cardiol. 2013;20(1):27–37.
13. Ferreira MJ, Cunha MJ, Albuquerque A, Moreira AP, Ramos D, Costa G, et al. Prognosis of normal stress-only gated-SPECT myocardial perfusion imaging: a single center study. Int J Cardiovasc Imaging. 2013;29(7):1639–44.
14. Gowd BM, Heller GV, Parker MW. Stress-only SPECT myocardial perfusion imaging: a review. J Nucl Cardiol. 2014;21(6):1200–12.
15. Dilsizian V, Bonow RO. Current diagnostic techniques of assessing myocardial viability in patients with hibernating and stunned myocardium. Circulation. 1993;87(1):1–20.
16. Dilsizian V. Transition from SPECT to PET myocardial perfusion imaging: a desirable change in nuclear cardiology to approach perfection. J Nucl Cardiol. 2016;23(3):337–8.
17. Bateman TM. Advantages and disadvantages of PET and SPECT in a busy clinical practice. J Nucl Cardiol. 2012;19(Suppl 1):S3–11.
18. Stabin MG. Radiopharmaceuticals for nuclear cardiology: radiation dosimetry, uncertainties, and risk. J Nucl Med. 2008;49(9):1555–63.
19. Maddahi J, Packard RR. Cardiac PET perfusion tracers: current status and future directions. Semin Nucl Med. 2014;44(5):333–43.
20. Nakazato R, Berman DS, Alexanderson E, Slomka P. Myocardial perfusion imaging with PET. Imaging Med. 2013;5(1):35–46.
21. Cerqueira MD. Pharmacologic stress versus maximal-exercise stress for perfusion imaging: which, when, and why? J Nucl Cardiol. 1996;3(6 Pt 2):S10–4.
22. Iskandrian AS, Heo J, Kong B, Lyons E. Effect of exercise level on the ability of thallium-201 tomographic imaging in detecting coronary artery disease: analysis of 461 patients. J Am Coll Cardiol. 1989;14(6):1477–86.
23. Cerqueira MD. The future of pharmacologic stress: selective A2A adenosine receptor agonists. Am J Cardiol. 2004;94(2A):33D–40D. discussion D-2D
24. Cerqueira MD, Verani MS, Schwaiger M, Heo J, Iskandrian AS. Safety profile of adenosine stress perfusion imaging: results from the Adenoscan multicenter trial registry. J Am Coll Cardiol. 1994;23(2):384–9.
25. Ranhosky A, Kempthorne-Rawson J. The safety of intravenous dipyridamole thallium myocardial perfusion imaging. Intravenous dipyridamole thallium imaging study group. Circulation. 1990;81(4):1205–9.
26. Mahmarian JJ, Cerqueira MD, Iskandrian AE, Bateman TM, Thomas GS, Hendel RC, et al. Regadenoson induces comparable left ventricular perfusion defects as adenosine: a quantitative analysis from the ADVANCE MPI 2 trial. J Am Coll Cardiol Img. 2009;2(8):959–68.
27. Hendel RC, Bateman TM, Cerqueira MD, Iskandrian AE, Leppo JA, Blackburn B, et al. Initial clinical experience with regadenoson, a novel selective A2A agonist for pharmacologic stress single-photon emission computed tomography myocardial perfusion imaging. J Am Coll Cardiol. 2005;46(11):2069–75.
28. Al Jaroudi W, Iskandrian AE. Regadenoson: a new myocardial stress agent. J Am Coll Cardiol. 2009;54(13):1123–30.
29. Lette J, Tatum J, Fraser S, Miller D, Waters D, Heller G, et al. Safety of dipyridamole testing in 73,806 patients: the multicenter dipyridamole safety study. J Nucl Cardiol. 1995;2(1):3–17.
30. Leppo JA. Comparison of pharmacologic stress agents. J Nucl Cardiol. 1996;3(6 Pt 2):S22–6.
31. American Society of Nuclear Cardiology. Updated imaging guidelines for nuclear cardiology procedures, part 1. J Nucl Cardiol. 2001;8(1):G5–G58.
32. Hays JT, Mahmarian JJ, Cochran AJ, Verani MS. Dobutamine thallium-201 tomography for evaluating patients with suspected coronary artery disease unable to undergo exercise or vasodilator pharmacologic stress testing. J Am Coll Cardiol. 1993;21(7):1583–90.
33. Agostini D, Marie PY, Ben-Haim S, Rouzet F, Songy B, Giordano A, et al. Performance of cardiac cadmium-zinc-telluride gamma camera imaging in coronary artery disease: a review from the cardiovascular committee of the European Association of Nuclear Medicine (EANM). Eur J Nucl Med Mol Imaging. 2016;43(13):2423–32.
34. Nudi F, Iskandrian AE, Schillaci O, Peruzzi M, Frati G, Biondi-Zoccai G. Diagnostic accuracy of myocardial perfusion imaging with CZT technology: systemic review and meta-analysis of comparison with invasive coronary angiography. J Am Coll Cardiol Img. 2017;10(7):787–94.
35. Germano G, Kiat H, Kavanagh PB, Moriel M, Mazzanti M, Su HT, et al. Automatic quantification of ejection fraction from gated myocardial perfusion SPECT. J Nucl Med. 1995;36(11):2138–47.

36. Akincioglu C, Berman DS, Nishina H, Kavanagh PB, Slomka PJ, Abidov A, et al. Assessment of diastolic function using 16-frame 99mTc-sestamibi gated myocardial perfusion SPECT: normal values. J Nucl Med. 2005;46(7):1102–8.
37. Choi JY, Lee KH, Kim SJ, Kim SE, Kim BT, Lee SH, et al. Gating provides improved accuracy for differentiating artifacts from true lesions in equivocal fixed defects on technetium 99m tetrofosmin perfusion SPECT. J Nucl Cardiol. 1998;5(4):395–401.
38. Everaert H, Franken PR, Flamen P, Goris M, Momen A, Bossuyt A. Left ventricular ejection fraction from gated SPET myocardial perfusion studies: a method based on the radial distribution of count rate density across the myocardial wall. Eur J Nucl Med. 1996;23(12):1628–33.
39. Everaert H, Vanhove C, Franken PR. Gated SPET myocardial perfusion acquisition within 5 minutes using focussing collimators and a three-head gamma camera. Eur J Nucl Med. 1998;25(6):587–93.
40. Gunning MG, Anagnostopoulos C, Davies G, Forbat SM, Ell PJ, Underwood SR. Gated technetium-99m-tetrofosmin SPECT and cine MRI to assess left ventricular contraction. J Nucl Med. 1997;38(3):438–42.
41. Mochizuki T, Murase K, Tanaka H, Kondoh T, Hamamoto K, Tauxe WN. Assessment of left ventricular volume using ECG-gated SPECT with technetium-99m-MIBI and technetium-99m-tetrofosmin. J Nucl Med. 1997;38(1):53–7.
42. Slomka PJ, Berman DS, Xu Y, Kavanagh P, Hayes SW, Dorbala S, et al. Fully automated wall motion and thickening scoring system for myocardial perfusion SPECT: method development and validation in large population. J Nucl Cardiol. 2012;19(2):291–302.
43. Abidov A, Germano G, Hachamovitch R, Slomka P, Berman DS. Gated SPECT in assessment of regional and global left ventricular function: an update. J Nucl Cardiol. 2013;20(6):1118–43. quiz 44-6
44. Dorbala S, Di Carli MF, Delbeke D, Abbara S, DePuey EG, Dilsizian V, et al. SNMMI/ASNC/SCCT guideline for cardiac SPECT/CT and PET/CT 1.0. J Nucl Med. 2013;54(8):1485–507.
45. Gaemperli O, Kaufmann PA, Alkadhi H. Cardiac hybrid imaging. Eur J Nucl Med Mol Imaging. 2014;41(Suppl 1):S91–103.
46. Schaap J, de Groot JA, Nieman K, Meijboom WB, Boekholdt SM, Kauling RM, et al. Added value of hybrid myocardial perfusion SPECT and CT coronary angiography in the diagnosis of coronary artery disease. Eur Heart J Cardiovasc Imaging. 2014;15(11):1281–8.
47. Cerqueira MD, Weissman NJ, Dilsizian V, Jacobs AK, Kaul S, Laskey WK, et al. Standardized myocardial segmentation and nomenclature for tomographic imaging of the heart. A statement for healthcare professionals from the cardiac imaging Committee of the Council on clinical cardiology of the American Heart Association. Int J Cardiovasc Imaging. 2002;18(1):539–42.
48. Xu Y, Kavanagh P, Fish M, Gerlach J, Ramesh A, Lemley M, et al. Automated quality control for segmentation of myocardial perfusion SPECT. J Nucl Med. 2009;50(9):1418–26.
49. Slomka PJ, Nishina H, Berman DS, Akincioglu C, Abidov A, Friedman JD, et al. Automated quantification of myocardial perfusion SPECT using simplified normal limits. J Nucl Cardiol. 2005;12(1):66–77.
50. Slomka P, Xu Y, Berman D, Germano G. Quantitative analysis of perfusion studies: strengths and pitfalls. J Nucl Cardiol. 2012;19(2):338–46.
51. Ziadi MC. Myocardial flow reserve (MFR) with positron emission tomography (PET)/computed tomography (CT): clinical impact in diagnosis and prognosis. Cardiovasc diagn Ther. 2017;7(2):206–18.
52. Cerqueira MD. The user-friendly nuclear cardiology report: what needs to be considered and what is included. J Nucl Cardiol. 1996;3(4):350–5.
53. Hendel RC, Wackers FJ, Berman DS, Ficaro E, Depuey EG, Klein L, et al. American society of nuclear cardiology consensus statement: reporting of radionuclide myocardial perfusion imaging studies. J Nucl Cardiol. 2003;10(6):705–8.
54. Tragardh E, Hesse B, Knuuti J, Flotats A, Kaufmann PA, Kitsiou A, et al. Reporting nuclear cardiology: a joint position paper by the European Association of Nuclear Medicine (EANM) and the European Association of Cardiovascular Imaging (EACVI). Eur Heart J Cardiovasc Imaging. 2015;16(3):272–9.
55. Tilkemeier PL, Bourque J, Doukky R, Sanghani R, Weinberg RL. ASNC imaging guidelines for nuclear cardiology procedures : standardized reporting of nuclear cardiology procedures. J Nucl Cardiol. 2017;24:2064.
56. Iskandrian AE, Heo J, Nallamothu N. Detection of coronary artery disease in women with use of stress single-photon emission computed tomography myocardial perfusion imaging. J Nucl Cardiol. 1997;4(4):329–35.
57. Mahmarian JJ, Boyce TM, Goldberg RK, Cocanougher MK, Roberts R, Verani MS. Quantitative exercise thallium-201 single photon emission computed tomography for the enhanced diagnosis of ischemic heart disease. J Am Coll Cardiol. 1990;15(2):318–29.
58. Fleischmann KE, Hunink MG, Kuntz KM, Douglas PS. Exercise echocardiography or exercise SPECT imaging? A meta-analysis of diagnostic test performance. JAMA. 1998;280(10):913–20.
59. Parker MW, Iskandar A, Limone B, Perugini A, Kim H, Jones C, et al. Diagnostic accuracy of cardiac positron emission tomography versus single photon emission computed tomography for coronary artery disease: a bivariate meta-analysis. Circ Cardiovasc Imaging. 2012;5(6):700–7.
60. Lee JM, Kim CH, Koo BK, Hwang D, Park J, Zhang J, et al. Integrated myocardial perfusion imaging diagnostics improve detection of functionally significant coronary artery stenosis by 13N-ammonia

positron emission tomography. Circ Cardiovasc Imaging. 2016;9(9):pii: e004768.
61. Sciagra R, Passeri A, Bucerius J, Verberne HJ, Slart RH, Lindner O, et al. Clinical use of quantitative cardiac perfusion PET: rationale, modalities and possible indications. Position paper of the cardiovascular Committee of the European Association of nuclear medicine (EANM). Eur J Nucl Med Mol Imaging. 2016;43(8):1530–45.
62. Hendel RC, Berman DS, Di Carli MF, Heidenreich PA, Henkin RE, Pellikka PA, et al. ACCF/ASNC/ACR/AHA/ASE/SCCT/SCMR/SNM 2009 appropriate use criteria for cardiac radionuclide imaging: a report of the American College of Cardiology Foundation appropriate use criteria task force, the American Society of Nuclear Cardiology, the American College of Radiology, the American Heart Association, the American Society of Echocardiography, the Society of Cardiovascular Computed Tomography, the Society for Cardiovascular Magnetic Resonance, and the Society of Nuclear Medicine. J Am Coll Cardiol. 2009;53(23):2201–29.
63. Task Force M, Montalescot G, Sechtem U, Achenbach S, Andreotti F, Arden C, et al. 2013 ESC guidelines on the management of stable coronary artery disease: the Task Force on the management of stable coronary artery disease of the European Society of Cardiology. Eur Heart J. 2013;34(38):2949–3003.
64. Gibbons RJ, Balady GJ, Bricker JT, Chaitman BR, Fletcher GF, Froelicher VF, et al. ACC/AHA 2002 guideline update for exercise testing: summary article. A report of the American College of Cardiology/American Heart Association Task Force on practice guidelines (committee to update the 1997 exercise testing guidelines). J Am Coll Cardiol. 2002;40(8):1531–40.
65. Hachamovitch R, Berman DS, Shaw LJ, Kiat H, Cohen I, Cabico JA, et al. Incremental prognostic value of myocardial perfusion single photon emission computed tomography for the prediction of cardiac death: differential stratification for risk of cardiac death and myocardial infarction. Circulation. 1998;97(6):535–43.
66. Shaw LJ, Hachamovitch R, Peterson ED, Lewin HC, Iskandrian AE, Miller DD, et al. Using an outcomes-based approach to identify candidates for risk stratification after exercise treadmill testing. J Gen Intern Med. 1999;14(1):1–9.
67. Gibbons RJ, Hodge DO, Berman DS, Akinboboye OO, Heo J, Hachamovitch R, et al. Long-term outcome of patients with intermediate-risk exercise electrocardiograms who do not have myocardial perfusion defects on radionuclide imaging. Circulation. 1999;100(21):2140–5.
68. Gibbons RJ, Abrams J, Chatterjee K, Daley J, Deedwania PC, Douglas JS, et al. ACC/AHA 2002 guideline update for the management of patients with chronic stable angina--summary article: a report of the American College of Cardiology/American Heart Association Task Force on practice guidelines (committee on the Management of Patients with Chronic Stable Angina). J Am Coll Cardiol. 2003;41(1):159–68.
69. Akinboboye OO, Idris O, Onwuanyi A, Berekashvili K, Bergmann SR. Incidence of major cardiovascular events in black patients with normal myocardial stress perfusion study results. J Nucl Cardiol. 2001;8(5):541–7.
70. Shaw LJ, Hendel RC, Cerquiera M, Mieres JH, Alazraki N, Krawczynska E, et al. Ethnic differences in the prognostic value of stress technetium-99m tetrofosmin gated single-photon emission computed tomography myocardial perfusion imaging. J Am Coll Cardiol. 2005;45(9):1494–504.
71. Alkeylani A, Miller DD, Shaw LJ, Travin MI, Stratmann HG, Jenkins R, et al. Influence of race on the prediction of cardiac events with stress technetium-99m sestamibi tomographic imaging in patients with stable angina pectoris. Am J Cardiol. 1998;81(3):293–7.
72. Shaw LJ, Bairey Merz CN, Pepine CJ, Reis SE, Bittner V, Kelsey SF, et al. Insights from the NHLBI-sponsored Women's ischemia syndrome evaluation (WISE) study: part I: gender differences in traditional and novel risk factors, symptom evaluation, and gender-optimized diagnostic strategies. J Am Coll Cardiol. 2006;47(3 Suppl):S4–S20.
73. Iskandar A, Limone B, Parker MW, Perugini A, Kim H, Jones C, et al. Gender differences in the diagnostic accuracy of SPECT myocardial perfusion imaging: a bivariate meta-analysis. J Nucl Cardiol. 2013;20(1):53–63.
74. Phillips LM, Mieres JH. Noninvasive assessment of coronary artery disease in women: what's next? Curr Cardiol Rep. 2010;12(2):147–54.
75. Patel MB, Bui LP, Kirkeeide RL, Gould KL. Imaging microvascular dysfunction and mechanisms for female-male differences in CAD. J Am Coll Cardiol Img. 2016;9(4):465–82.
76. Campisi R, Marengo FD. Coronary microvascular dysfunction in women with nonobstructive ischemic heart disease as assessed by positron emission tomography. Cardiovasc Diagn Ther. 2017;7(2):196–205.
77. Wagdy HM, Hodge D, Christian TF, Miller TD, Gibbons RJ. Prognostic value of vasodilator myocardial perfusion imaging in patients with left bundle-branch block. Circulation. 1998;97(16):1563–70.
78. Gioia G, Bagheri B, Gottlieb CD, Schwartzman DS, Callans DJ, Marchlinski FE, et al. Prediction of outcome of patients with life-threatening ventricular arrhythmias treated with automatic implantable cardioverter-defibrillators using SPECT perfusion imaging. Circulation. 1997;95(2):390–4.
79. Amanullah AM, Berman DS, Kang X, Cohen I, Germano G, Friedman JD. Enhanced prognostic stratification of patients with left ventricular hypertrophy with the use of single-photon emission computed tomography. Am Heart J. 2000;140(3):456–62.

80. Elhendy A, van Domburg RT, Sozzi FB, Poldermans D, Bax JJ, Roelandt JR. Impact of hypertension on the accuracy of exercise stress myocardial perfusion imaging for the diagnosis of coronary artery disease. Heart. 2001;85(6):655–61.
81. Bartram P, Toft J, Hanel B, Ali S, Gustafsson F, Mortensen J, et al. False-positive defects in technetium-99m sestamibi myocardial single-photon emission tomography in healthy athletes with left ventricular hypertrophy. Eur J Nucl Med. 1998;25(9):1308–12.
82. Blumenthal RS, Becker DM, Moy TF, Coresh J, Wilder LB, Becker LC. Exercise thallium tomography predicts future clinically manifest coronary heart disease in a high-risk asymptomatic population. Circulation. 1996;93(5):915–23.
83. Blumenthal RS, Becker DM, Yanek LR, Aversano TR, Moy TF, Kral BG, et al. Detecting occult coronary disease in a high-risk asymptomatic population. Circulation. 2003;107(5):702–7.
84. American Diabetes Association. Diabetes mellitus: a major risk factor for cardiovascular disease. A joint editorial statement by the American Diabetes Association; The National Heart, Lung, and Blood Institute; The Juvenile Diabetes Foundation International; The National Institute of Diabetes and Digestive and Kidney Diseases; and The American Heart Association. Circulation. 1999;100(10):1132–3.
85. Giri S, Shaw LJ, Murthy DR, Travin MI, Miller DD, Hachamovitch R, et al. Impact of diabetes on the risk stratification using stress single-photon emission computed tomography myocardial perfusion imaging in patients with symptoms suggestive of coronary artery disease. Circulation. 2002;105(1):32–40.
86. Kang X, Berman DS, Lewin H, Miranda R, Erel J, Friedman JD, et al. Comparative ability of myocardial perfusion single-photon emission computed tomography to detect coronary artery disease in patients with and without diabetes mellitus. Am Heart J. 1999;137(5):949–57.
87. Kang X, Berman DS, Lewin HC, Cohen I, Friedman JD, Germano G, et al. Incremental prognostic value of myocardial perfusion single photon emission computed tomography in patients with diabetes mellitus. Am Heart J. 1999;138(6 Pt 1):1025–32.
88. Wackers FJ, Young LH, Inzucchi SE, Chyun DA, Davey JA, Barrett EJ, et al. Detection of silent myocardial ischemia in asymptomatic diabetic subjects: the DIAD study. Diabetes Care. 2004;27(8):1954–61.
89. Young LH, Wackers FJ, Chyun DA, Davey JA, Barrett EJ, Taillefer R, et al. Cardiac outcomes after screening for asymptomatic coronary artery disease in patients with type 2 diabetes: the DIAD study: a randomized controlled trial. JAMA. 2009;301(15):1547–55.
90. Amsterdam EA, Kirk JD, Bluemke DA, Diercks D, Farkouh ME, Garvey JL, et al. Testing of low-risk patients presenting to the emergency department with chest pain: a scientific statement from the American Heart Association. Circulation. 2010;122(17):1756–76.
91. Tatum JL, Jesse RL, Kontos MC, Nicholson CS, Schmidt KL, Roberts CS, et al. Comprehensive strategy for the evaluation and triage of the chest pain patient. Ann Emerg Med. 1997;29(1):116–25.
92. Heller GV, Stowers SA, Hendel RC, Herman SD, Daher E, Ahlberg AW, et al. Clinical value of acute rest technetium-99m tetrofosmin tomographic myocardial perfusion imaging in patients with acute chest pain and nondiagnostic electrocardiograms. J Am Coll Cardiol. 1998;31(5):1011–7.
93. Udelson JE, Beshansky JR, Ballin DS, Feldman JA, Griffith JL, Handler J, et al. Myocardial perfusion imaging for evaluation and triage of patients with suspected acute cardiac ischemia: a randomized controlled trial. JAMA. 2002;288(21):2693–700.
94. Brown KA, Rowen M. Prognostic value of a normal exercise myocardial perfusion imaging study in patients with angiographically significant coronary artery disease. Am J Cardiol. 1993;71(10):865–7.
95. Shaw LJ, Hachamovitch R, Berman DS, Marwick TH, Lauer MS, Heller GV, et al. The economic consequences of available diagnostic and prognostic strategies for the evaluation of stable angina patients: an observational assessment of the value of precatheterization ischemia. Economics of noninvasive diagnosis (END) multicenter study group. J Am Coll Cardiol. 1999;33(3):661–9.
96. Brindis RG, Douglas PS, Hendel RC, Peterson ED, Wolk MJ, Allen JM, et al. ACCF/ASNC appropriateness criteria for single-photon emission computed tomography myocardial perfusion imaging (SPECT MPI): a report of the American College of Cardiology Foundation quality strategic directions committee appropriateness criteria working group and the American Society of Nuclear Cardiology endorsed by the American Heart Association. J Am Coll Cardiol. 2005;46(8):1587–605.
97. McPherson JA, Robinson PS, Powers ER, Sarembock IJ, Gimple LW, Ragosta M. Angiographic findings in patients undergoing catheterization for recurrent symptoms within 30 days of successful coronary intervention. Am J Cardiol. 1999;84(5):589–92. A8
98. Jain A, Mahmarian JJ, Borges-Neto S, Johnston DL, Cashion WR, Lewis JM, et al. Clinical significance of perfusion defects by thallium-201 single photon emission tomography following oral dipyridamole early after coronary angioplasty. J Am Coll Cardiol. 1988;11(5):970–6.
99. Ho KT, Miller TD, Holmes DR, Hodge DO, Gibbons RJ. Long-term prognostic value of Duke treadmill score and exercise thallium-201 imaging performed one to three years after percutaneous transluminal coronary angioplasty. Am J Cardiol. 1999;84(11):1323–7.
100. Hamilos MI, Ostojic M, Beleslin B, Sagic D, Mangovski L, Stojkovic S, et al. Differential effects of drug-eluting stents on local endothelium-

dependent coronary vasomotion. J Am Coll Cardiol. 2008;51(22):2123–9.
101. Ertas G, van Beusekom HM, van der Giessen WJ. Late stent thrombosis, endothelialisation and drug-eluting stents. Netherlands Jeart J. 2009;17(4):177–80.
102. Miller TD, Christian TF, Hodge DO, Mullan BP, Gibbons RJ. Prognostic value of exercise thallium-201 imaging performed within 2 years of coronary artery bypass graft surgery. J Am Coll Cardiol. 1998;31(4):848–54.
103. Palmas W, Bingham S, Diamond GA, Denton TA, Kiat H, Friedman JD, et al. Incremental prognostic value of exercise thallium-201 myocardial single-photon emission computed tomography late after coronary artery bypass surgery. J Am Coll Cardiol. 1995;25(2):403–9.
104. Zellweger MJ, Lewin HC, Lai S, Dubois EA, Friedman JD, Germano G, et al. When to stress patients after coronary artery bypass surgery? Risk stratification in patients early and late post-CABG using stress myocardial perfusion SPECT: implications of appropriate clinical strategies. J Am Coll Cardiol. 2001;37(1):144–52.
105. Lauer MS, Lytle B, Pashkow F, Snader CE, Marwick TH. Prediction of death and myocardial infarction by screening with exercise-thallium testing after coronary-artery-bypass grafting. Lancet. 1998;351(9103):615–22.
106. Nallamothu N, Johnson JH, Bagheri B, Heo J, Iskandrian AE. Utility of stress single-photon emission computed tomography (SPECT) perfusion imaging in predicting outcome after coronary artery bypass grafting. Am J Cardiol. 1997;80(12):1517–21.
107. Eagle KA, Berger PB, Calkins H, Chaitman BR, Ewy GA, Fleischmann KE, et al. ACC/AHA guideline update for perioperative cardiovascular evaluation for noncardiac surgery--executive summary: a report of the American College of Cardiology/American Heart Association Task Force on practice guidelines (committee to update the 1996 guidelines on perioperative cardiovascular evaluation for noncardiac surgery). J Am Coll Cardiol. 2002;39(3):542–53.
108. Mangano DT, Goldman L. Preoperative assessment of patients with known or suspected coronary disease. N Engl J Med. 1995;333(26):1750–6.
109. Fleisher LA, Fleischmann KE, Auerbach AD, Barnason SA, Beckman JA, Bozkurt B, et al. 2014 ACC/AHA guideline on perioperative cardiovascular evaluation and management of patients undergoing noncardiac surgery: executive summary: a report of the American College of Cardiology/American Heart Association Task Force on practice guidelines. Developed in collaboration with the American College of Surgeons, American Society of Anesthesiologists, American Society of Echocardiography, American Society of Nuclear Cardiology, Heart Rhythm Society, Society for Cardiovascular Angiography and Interventions, Society of Cardiovascular Anesthesiologists, and Society of Vascular Medicine Endorsed by the Society of Hospital Medicine. J Nucl Cardiol. 2015;22(1):162–215.
110. Kristensen SD, Knuuti J, Saraste A, Anker S, Botker HE, Hert SD, et al. 2014 ESC/ESA guidelines on non-cardiac surgery: cardiovascular assessment and management: the joint Task Force on non-cardiac surgery: cardiovascular assessment and management of the European Society of Cardiology (ESC) and the European Society of Anaesthesiology (ESA). Eur Heart J. 2014;35(35):2383–431.
111. Rahimtoola SH. Chronic myocardial hibernation. Circulation. 1994;89(4):1907–8.
112. Patel H, Mazur W, Williams KA Sr, Kalra DK. Myocardial viability-state of the art: is it still relevant and how to best assess it with imaging? Trends Cardiovasc Med. 2018;28(1):24–37.
113. Acampa W, Cuocolo A, Petretta M, Bruno A, Castellani M, Finzi A, et al. Tetrofosmin imaging in the detection of myocardial viability in patients with previous myocardial infarction: comparison with sestamibi and Tl-201 scintigraphy. J Nucl Cardiol. 2002;9(1):33–40.
114. Orlandini A, Castellana N, Pascual A, Botto F, Cecilia Bahit M, Chacon C, et al. Myocardial viability for decision-making concerning revascularization in patients with left ventricular dysfunction and coronary artery disease: a meta-analysis of non-randomized and randomized studies. Int J Cardiol. 2015;182:494–9.
115. Di Carli MF, Davidson M, Little R, Khanna S, Mody FV, Brunken RC, et al. Value of metabolic imaging with positron emission tomography for evaluating prognosis in patients with coronary artery disease and left ventricular dysfunction. Am J Cardiol. 1994;73(8):527–33.
116. Di Carli MF, Asgarzadie F, Schelbert HR, Brunken RC, Laks H, Phelps ME, et al. Quantitative relation between myocardial viability and improvement in heart failure symptoms after revascularization in patients with ischemic cardiomyopathy. Circulation. 1995;92(12):3436–44.
117. Allman KC, Shaw LJ, Hachamovitch R, Udelson JE. Myocardial viability testing and impact of revascularization on prognosis in patients with coronary artery disease and left ventricular dysfunction: a meta-analysis. J Am Coll Cardiol. 2002;39(7):1151–8.
118. Beanlands RS, Ruddy TD, de Kemp RA, Iwanochko RM, Coates G, Freeman M, et al. Positron emission tomography and recovery following revascularization (PARR-1): the importance of scar and the development of a prediction rule for the degree of recovery of left ventricular function. J Am Coll Cardiol. 2002;40(10):1735–43.
119. D'Egidio G, Nichol G, Williams KA, Guo A, Garrard L, de Kemp RA, et al. Increasing benefit from revascularization is associated with increasing amounts of myocardial hibernation: a substudy of the PARR-2 trial. J Am Coll Cardiol Img. 2009;2(9):1060–8.

120. Hesse B, Lindhardt TB, Acampa W, Anagnostopoulos C, Ballinger J, Bax JJ, et al. EANM/ESC guidelines for radionuclide imaging of cardiac function. Eur J Nucl Med Mol Imaging. 2008;35(4):851–85.
121. Gibbons RJ. Rest and exercise radionuclide angiography for diagnosis in chronic ischemic heart disease. Circulation. 1991;84(3 Suppl):I93–9.
122. Schwartz RG, McKenzie WB, Alexander J, Sager P, D'Souza A, Manatunga A, et al. Congestive heart failure and left ventricular dysfunction complicating doxorubicin therapy. Seven-year experience using serial radionuclide angiocardiography. Am J Med. 1987;82(6):1109–18.
123. Schwartz RG, Jain D, Storozynsky E. Traditional and novel methods to assess and prevent chemotherapy-related cardiac dysfunction noninvasively. J Nucl Cardiol. 2013;20(3):443–64.
124. Zamorano JL, Lancellotti P, Rodriguez Munoz D, Aboyans V, Asteggiano R, Galderisi M, et al. 2016 ESC position paper on cancer treatments and cardiovascular toxicity developed under the auspices of the ESC Committee for practice guidelines: the Task Force for cancer treatments and cardiovascular toxicity of the European Society of Cardiology (ESC). Eur Heart J. 2016;37(36):2768–801.
125. Bloom MW, Hamo CE, Cardinale D, Ky B, Nohria A, Baer L, et al. Cancer therapy-related cardiac dysfunction and heart failure: part 1: definitions, pathophysiology, risk factors, and imaging. Circ Heart Fail. 2016;9(1):e002661.
126. Hamo CE, Bloom MW, Cardinale D, Ky B, Nohria A, Baer L, et al. Cancer therapy-related cardiac dysfunction and heart failure: part 2: prevention, treatment, guidelines, and future directions. Circ Heart Fail. 2016;9(2):e002843.
127. Verberne HJ, Brewster LM, Somsen GA, van Eck-Smit BL. Prognostic value of myocardial 123I-metaiodobenzylguanidine (MIBG) parameters in patients with heart failure: a systematic review. Eur Heart J. 2008;29(9):1147–59.
128. Jacobson AF, Senior R, Cerqueira MD, Wong ND, Thomas GS, Lopez VA, et al. Myocardial iodine-123 meta-iodobenzylguanidine imaging and cardiac events in heart failure. Results of the prospective ADMIRE-HF (AdreView myocardial imaging for risk evaluation in heart failure) study. J Am Coll Cardiol. 2010;55(20):2212–21.
129. Fallavollita JA, Heavey BM, Luisi AJ Jr, Michalek SM, Baldwa S, Mashtare TL Jr, et al. Regional myocardial sympathetic denervation predicts the risk of sudden cardiac arrest in ischemic cardiomyopathy. J Am Coll Cardiol. 2014;63(2):141–9.
130. Bejar D, Colombo PC, Latif F, Yuzefpolskaya M. Infiltrative cardiomyopathies. Clin Med Insights Cardiol. 2015;9(Suppl 2):29–38.
131. Juneau D, Erthal F, Alzahrani A, Alenazy A, Nery PB, Beanlands RS, et al. Systemic and inflammatory disorders involving the heart: the role of PET imaging. Q J Nucl Med Mol Imaging. 2016;60(4):383–96.
132. Erthal F, Juneau D, Lim SP, Dwivedi G, Nery PB, Birnie D, et al. Imaging of cardiac sarcoidosis. Q J Nucl Med Mol Imaging. 2016;60(3):252–63.
133. Ahmadian A, Pawar S, Govender P, Berman J, Ruberg FL, Miller EJ. The response of FDG uptake to immunosuppressive treatment on FDG PET/CT imaging for cardiac sarcoidosis. J Nucl Cardiol. 2017;24(2):413–24.
134. Chareonthaitawee P, Beanlands RS, Chen W, Dorbala S, Miller EJ, Murthy VL, et al. Joint SNMMI-ASNC expert consensus document on the role of 18F-FDG PET/CT in cardiac sarcoid detection and therapy monitoring. J Nucl Cardiol. 2017;24:1741.
135. Bokhari S, Shahzad R, Castano A, Maurer MS. Nuclear imaging modalities for cardiac amyloidosis. J Nucl Cardiol. 2014;21(1):175–84.
136. Habib G, Lancellotti P, Antunes MJ, Bongiorni MG, Casalta JP, Del Zotti F, et al. 2015 ESC guidelines for the management of infective endocarditis: the Task Force for the Management of Infective Endocarditis of the European Society of Cardiology (ESC). Endorsed by: European Association for Cardio-Thoracic Surgery (EACTS), the European Association of Nuclear Medicine (EANM). Eur Heart J. 2015;36(44):3075–128.
137. Baddour LM, Wilson WR, Bayer AS, Fowler VG Jr, Tleyjeh IM, Rybak MJ, et al. Infective endocarditis in adults: diagnosis, antimicrobial therapy, and Management of Complications: a scientific statement for healthcare professionals from the American Heart Association. Circulation. 2015;132(15):1435–86.
138. Gomes A, Glaudemans A, Touw DJ, van Melle JP, Willems TP, Maass AH, et al. Diagnostic value of imaging in infective endocarditis: a systematic review. Lancet Infect Dis. 2017;17(1):e1–e14.